

# Radiative Non-leptonic Kaon Decays

G. D'Ambrosio<sup>1</sup>, G. Ecker<sup>2</sup>, G. Isidori<sup>3</sup> and H. Neufeld<sup>2</sup>

<sup>1</sup>) Istituto Nazionale di Fisica Nucleare, Sezione di Napoli  
 Dipartimento di Scienze Fisiche, Università di Napoli  
 I-80125 Napoli, Italy

<sup>2</sup>) Institut für Theoretische Physik, Universität Wien  
 A-1090 Wien, Austria

<sup>3</sup>) Istituto Nazionale di Fisica Nucleare, Sezione di Roma  
 Dipartimento di Fisica, Università di Roma  
 I-00185 Roma, Italy

## Contents

|              |  |                |
|--------------|--|----------------|
| <b>1</b>     | <b>Non-leptonic weak interactions</b>                        | <b>266</b>     |
| 1.1          | Introduction . . . . .                                       | 266            |
| 1.2          | Chiral perturbation theory . . . . .                         | 267            |
| 1.3          | The chiral anomaly in the non-leptonic weak sector . . . . . | 272            |
| <br><b>2</b> | <br><b>Kaon decays with two photons in the final state</b>   | <br><b>274</b> |
| 2.1          | $K_S \rightarrow \gamma\gamma$ . . . . .                     | 275            |
| 2.2          | $K_L \rightarrow \pi^0\gamma\gamma$ . . . . .                | 276            |
| 2.3          | $K_L \rightarrow \gamma\gamma$ . . . . .                     | 281            |
| 2.4          | $K^+ \rightarrow \pi^+\gamma\gamma$ . . . . .                | 283            |
| 2.5          | $K_S \rightarrow \pi^0\gamma\gamma$ . . . . .                | 284            |

---

<sup>1</sup>Supported by the INFN, by the EC under the HCM contract number CHRX-CT920026 and by the authors home institutions

|          |  |            |
|----------|--|------------|
| 2.6      | $K_{L,S} \rightarrow \pi^0 \pi^0 \gamma \gamma$          | 286        |
| 2.7      | $K^+ \rightarrow \pi^+ \pi^0 \gamma \gamma$              | 286        |
| 2.8      | CP violation   | 287        |
| 2.9      | Improvements at DAΦNE                                    | 288        |
| <b>3</b> | <b>Kaon decays with one photon in the final state</b>    | <b>289</b> |
| 3.1      | Matrix elements and decay rates                          | 289        |
| 3.2      | Low's theorem and the chiral expansion                   | 289        |
| 3.3      | $K_{L,S} \rightarrow \pi^0 \pi^0 \gamma$                 | 290        |
| 3.4      | $K_S \rightarrow \pi^+ \pi^- \gamma$                     | 290        |
| 3.5      | $K_L \rightarrow \pi^+ \pi^- \gamma$                     | 291        |
| 3.6      | $K^+ \rightarrow \pi^+ \pi^0 \gamma$                     | 294        |
| 3.7      | CP violation   | 296        |
| 3.8      | Improvements at DAΦNE                                    | 297        |
| <b>4</b> | <b>Kaon decays with a lepton pair in the final state</b> | <b>297</b> |
| 4.1      | No pions in the final state                              | 297        |
| 4.1.1    | $K^0 \rightarrow \gamma^* \gamma^*$                      | 297        |
| 4.1.2    | $K^0 \rightarrow l^+ l^-$                                | 300        |
| 4.2      | $K \rightarrow \pi l^+ l^-$                              | 302        |
| 4.3      | $K_L \rightarrow \pi^0 \pi^0 e^+ e^-$                    | 304        |
| 4.4      | CP violation   | 305        |
| 4.5      | Improvements at DAΦNE                                    | 306        |
| <b>A</b> | <b>Loop functions</b>                                    | <b>307</b> |

# 1 Non-leptonic weak interactions

## 1.1 Introduction

Many radiative non-leptonic kaon decays will be interesting by-products of the experimental program at DAΦNE. The following survey serves several purposes:

- We investigate to what extent DAΦNE will be able to test the Standard Model in the confinement regime with radiative kaon decays. We concentrate on processes which

can be detected at DAΦNE and we review briefly those decays where only upper limits can be expected <sup>2</sup>.

- With reliable predictions from the Standard Model at our disposal, one can set about looking for new physics. This applies especially to transitions that are either suppressed or forbidden in the Standard Model.
- Unambiguous predictions of the Standard Model can be made for the low-energy structure of non-leptonic weak amplitudes. Chiral perturbation theory (CHPT) allows to specify this low-energy structure in terms of some a priori undetermined low-energy constants. All specific models for the non-leptonic weak transitions have to satisfy those low-energy theorems, but they can be expected to produce more detailed predictions for the low-energy constants.

We collect the decays of interest for DAΦNE in Table 1. We have used the average experimental rates from Ref. [2]. Some of the theoretical estimates are based on model assumptions that go beyond pure CHPT. More details on theory and experiments will be found in the relative sections. To illustrate the improvements at DAΦNE, we have assumed the following numbers of tagged events per year corresponding to a luminosity of  $5 \cdot 10^{32} \text{ s}^{-1} \text{ cm}^{-2}$  and an effective year of  $10^7 \text{ s}$  [3]:

$$1.1(1.7) \cdot 10^9 \text{ } K_L(K_S) \text{ , } \quad 9 \cdot 10^9 \text{ } K^\pm \text{ .} \quad (1.1)$$

Furthermore, for channels with experimental limits only or with poor statistics, we have used the theoretical predictions to estimate the number of events expected at DAΦNE.

We have classified the radiative non-leptonic decays in Table 1 in the following groups:

- i.* Two photons in the final state;
- ii.* One photon in the final state, distinguishing between internal bremsstrahlung and direct emission;
- iii.* Decays with a lepton pair.

We also discuss some possible bounds that can be put on CP violating quantities with radiative non-leptonic decays at DAΦNE.

## 1.2 Chiral perturbation theory

CHPT for the non-leptonic weak interactions is a straightforward extension of the standard CHPT formalism for the strong, electromagnetic and semileptonic weak interactions (for a general introduction and additional references we refer to [4]). The  $\Delta S = 1$  non-leptonic

---

<sup>2</sup>There are several recent reviews of rare  $K$  decays [1] which can be consulted for additional information.

| channel  | $BR_{\text{exp}}$               | $BR_{\text{theor}}$    | # events/yr           |
|--|---------------------------------|------------------------|-----------------------|
| Two photons in the final state.  |                                 |                        |                       |
| $K_S \rightarrow \gamma\gamma$   | $(2.4 \pm 1.2) \cdot 10^{-6}$   | $2.1 \cdot 10^{-6}$    | $3.6 \cdot 10^3$      |
| $K_L \rightarrow \gamma\gamma$   | $(5.73 \pm 0.27) \cdot 10^{-4}$ | $\sim 5 \cdot 10^{-4}$ | $6.3 \cdot 10^5$      |
| $K_L \rightarrow \pi^0\gamma\gamma$  | $(1.70 \pm 0.28) \cdot 10^{-6}$ | $\sim 10^{-6}$         | $1.9 \cdot 10^3$      |
| $K_S \rightarrow \pi^0\gamma\gamma$ ( $M_{\gamma\gamma} > 220 \text{ MeV}$ )               | —                               | $3.8 \cdot 10^{-8}$    | 65                    |
| $K^+ \rightarrow \pi^+\gamma\gamma$  | $< 1.5 \cdot 10^{-4}$           | $\sim 5 \cdot 10^{-7}$ | $\sim 4.5 \cdot 10^3$ |
| $K_L \rightarrow \pi^0\pi^0\gamma\gamma$ ( $ M_{\gamma\gamma} - M_\pi  > 20 \text{ MeV}$ ) | —                               | $3 \cdot 10^{-8}$      | 33                    |
| $K_S \rightarrow \pi^0\pi^0\gamma\gamma$ ( $ M_{\gamma\gamma} - M_\pi  > 20 \text{ MeV}$ ) | —                               | $5 \cdot 10^{-9}$      | 8                     |
| One photon in the final state, internal bremsstrahlung.                                    |                                 |                        |                       |
| $K_S \rightarrow \pi^+\pi^-\gamma$ ( $E_\gamma^* > 50 \text{ MeV}$ )                       | $(1.78 \pm 0.05) \cdot 10^{-3}$ | $1.75 \cdot 10^{-3}$   | $3 \cdot 10^6$        |
| $K_L \rightarrow \pi^+\pi^-\gamma$ ( $E_\gamma^* > 20 \text{ MeV}$ )                       | $(1.49 \pm 0.08) \cdot 10^{-5}$ | $1.42 \cdot 10^{-5}$   | $1.5 \cdot 10^4$      |
| $K^+ \rightarrow \pi^+\pi^0\gamma$ ( $T_c^* = (55-90) \text{ MeV}$ )                       | $(2.57 \pm 0.16) \cdot 10^{-4}$ | $2.61 \cdot 10^{-4}$   | $2.3 \cdot 10^6$      |
| One photon in the final state, direct emission.  |                                 |                        |                       |
| $K_S \rightarrow \pi^+\pi^-\gamma$ ( $E_\gamma^* > 50 \text{ MeV}$ )                       | $< 9 \cdot 10^{-5}$             | $\sim 10^{-6}$         | $\sim 1.7 \cdot 10^3$ |
| $K_L \rightarrow \pi^+\pi^-\gamma$ ( $E_\gamma^* > 20 \text{ MeV}$ )                       | $(3.19 \pm 0.16) \cdot 10^{-5}$ | $\sim 10^{-5}$         | $3.5 \cdot 10^4$      |
| $K^+ \rightarrow \pi^+\pi^0\gamma$ ( $T_c^* = (55-90) \text{ MeV}$ )                       | $(1.8 \pm 0.4) \cdot 10^{-5}$   | $\sim 10^{-5}$         | $1.6 \cdot 10^5$      |
| Lepton pair without pions.   |                                 |                        |                       |
| $K_L \rightarrow \mu^+\mu^-$   | $(7.4 \pm 0.4) \cdot 10^{-9}$   | $\sim 7 \cdot 10^{-9}$ | 8                     |
| $K_L \rightarrow \gamma e^+e^-$  | $(9.1 \pm 0.5) \cdot 10^{-6}$   | $9 \cdot 10^{-6}$      | $1.0 \cdot 10^4$      |
| $K_L \rightarrow \gamma \mu^+\mu^-$  | $(2.8 \pm 2.8) \cdot 10^{-7}$   | $3.6 \cdot 10^{-7}$    | $4.0 \cdot 10^2$      |
| $K_S \rightarrow \gamma e^+e^-$  | —                               | $3.4 \cdot 10^{-8}$    | 58                    |
| $K_L \rightarrow e^+e^-e^+e^-$   | $(3.9 \pm 0.7) \cdot 10^{-8}$   | —                      | 43                    |
| Lepton pair with pions.  |                                 |                        |                       |
| $K_S \rightarrow \pi^0 e^+e^-$   | $< 1.1 \cdot 10^{-6}$           | $> 5 \cdot 10^{-10}$   | $> 1$                 |
| $K_S \rightarrow \pi^0 \mu^+\mu^-$   | —                               | $> 10^{-10}$           | —                     |
| $K^+ \rightarrow \pi^+ e^+e^-$   | $(2.74 \pm 0.23) \cdot 10^{-7}$ | $\sim 3 \cdot 10^{-7}$ | $2.5 \cdot 10^3$      |
| $K^+ \rightarrow \pi^+ \mu^+\mu^-$   | $< 2.3 \cdot 10^{-7}$           | $6 \cdot 10^{-8}$      | $5.4 \cdot 10^2$      |
| $K_L \rightarrow \pi^+\pi^-e^+e^-$   | $< 2.5 \cdot 10^{-6}$           | $2.8 \cdot 10^{-7}$    | $3.1 \cdot 10^2$      |

Table 1: Radiative kaon decays of interest for DAΦNE.

weak interactions are treated as a perturbation of the strong chiral Lagrangian. We only consider weak amplitudes to first order in the weak interactions,  $O(G_F)$ .

The effective Hamiltonian for  $\Delta S = 1$  weak interactions at energies much smaller than  $M_W$  takes the form of an operator product expansion [5]

$$\mathcal{H}_{\text{eff}}^{\Delta S=1} = \frac{G_F}{\sqrt{2}} V_{ud} V_{us}^* \sum_i C_i Q_i + \text{h.c.} \quad (1.2)$$

in terms of four-quark operators  $Q_i$  and Wilson coefficients  $C_i$ . Under the chiral group  $SU(3)_L \times SU(3)_R$ , the effective Hamiltonian (1.2) transforms as

$$\mathcal{H}_{\text{eff}}^{\Delta S=1} \sim (8_L, 1_R) + (27_L, 1_R) . \quad (1.3)$$

Due to the Goldstone theorem, the effective chiral Lagrangian for the  $\Delta S = 1$  non-leptonic weak interactions starts at  $O(p^2)$ . The most general chiral Lagrangian of lowest order with the same transformation properties as (1.3) has the form <sup>3</sup>

$$\mathcal{L}_2^{\Delta S=1} = G_8 \langle \lambda L_\mu L^\mu \rangle + G_{27} \left( L_{\mu 23} L_{11}^\mu + \frac{2}{3} L_{\mu 21} L_{13}^\mu \right) + \text{h.c.}, \quad (1.4)$$

where

$$\lambda = (\lambda_6 - i\lambda_7)/2 , \quad L_\mu = iF^2 U^\dagger D_\mu U , \quad (1.5)$$

and  $\langle A \rangle$  denotes the trace of the matrix  $A$ . The chiral couplings  $G_8$  and  $G_{27}$  measure the strength of the two parts in the effective Hamiltonian (1.2) transforming as  $(8_L, 1_R)$  and  $(27_L, 1_R)$ , respectively, under chiral rotations. From  $K \rightarrow 2\pi$  decays one finds:

$$|G_8| \simeq 9 \cdot 10^{-6} \text{ GeV}^{-2}, \quad G_{27}/G_8 \simeq 1/18 . \quad (1.6)$$

The big difference between the two couplings is a manifestation of the  $|\Delta I| = 1/2$  rule.

The effective Lagrangian (1.4) gives rise to the current algebra relations between  $K \rightarrow 2\pi$  and  $K \rightarrow 3\pi$  amplitudes. However, for the radiative transitions under consideration the lowest-order amplitudes due to (1.4) are “trivial” in the following sense:

1. Non-leptonic  $K$  decay amplitudes with any number of real or virtual photons and with at most one pion in the final state vanish at  $O(p^2)$  [6, 7]:

$$A(K \rightarrow [\pi] \gamma^* \dots \gamma^*) = 0 \quad \text{at } O(p^2) . \quad (1.7)$$

2. The amplitudes for two pions and any number of real or virtual photons in the final state factorize at  $O(p^2)$  into the on-shell amplitude for the corresponding  $K \rightarrow \pi\pi$  decay and a generalized bremsstrahlung amplitude independent of the specific decay [8, 9, 10]:

$$A(K \rightarrow \pi\pi\gamma^* \dots \gamma^*) = A(K \rightarrow \pi\pi) A_{\text{brems}} . \quad (1.8)$$

---

<sup>3</sup>We use the same conventions as in [4].

3. A similar statement holds for the decays  $K \rightarrow 3\pi\gamma$ : the amplitude of  $O(p^2)$  is completely determined by the corresponding non-radiative decay  $K \rightarrow 3\pi$  [11]. We will not discuss these decays in any detail here.

Therefore, the non-trivial aspects of radiative non-leptonic kaon decays appear at  $O(p^4)$  only. Similarly to the strong sector, the non-leptonic weak amplitudes consist in general of several parts:

- i. Tree level amplitudes from the most general effective chiral Lagrangian  $\mathcal{L}_4^{\Delta S=1}$  of  $O(p^4)$  with the transformation properties (1.3).
- ii. One-loop amplitudes from diagrams with a single vertex of  $\mathcal{L}_2^{\Delta S=1}$  in the loop.
- iii. Reducible tree level amplitudes with a single vertex from  $\mathcal{L}_2^{\Delta S=1}$  and with a single vertex from the strong Lagrangian  $\mathcal{L}_4$  or from the anomaly (cf. [4]).
- iv. Reducible one-loop amplitudes, consisting of a strong loop diagram connected to a vertex of  $\mathcal{L}_2^{\Delta S=1}$  by a single meson line. A typical diagram of this type contains an external  $K-\pi$  or  $K-\eta$  transition, possibly with one or two photons (generalized “pole diagrams”). The calculation of such diagrams is simplified by a rediagonalization of the kinetic and mass terms of  $\mathcal{L}_2 + \mathcal{L}_2^{\Delta S=1}$  (“weak rotation” [6, 7]).

For the tree level amplitudes of  $O(p^4)$  we shall only consider the octet part. The corresponding Lagrangian can be written as [12, 13]

$$\mathcal{L}_4^{\Delta S=1} = G_8 F^2 \sum_i N_i W_i + \text{h.c.} \quad (1.9)$$

with dimensionless coupling constants  $N_i$  and octet operators  $W_i$ . Referring to Ref. [13] for the complete Lagrangian, we list in Table 2 only the terms relevant for radiative decays.

The non-leptonic weak loop amplitudes are in general divergent. As in the strong sector with the corresponding low-energy constants  $L_i$ , the weak constants  $N_i$  absorb the remaining divergences. Using dimensional regularization for the loop diagrams, the  $N_i$  are decomposed as

$$\begin{aligned} N_i &= N_i^r(\mu) + Z_i \Lambda(\mu) \\ \Lambda(\mu) &= \frac{\mu^{d-4}}{16\pi^2} \left\{ \frac{1}{d-4} - \frac{1}{2} [\ln(4\pi) + \Gamma'(1) + 1] \right\} \end{aligned} \quad (1.10)$$

with an arbitrary scale parameter  $\mu$ . The constants  $Z_i$  listed in Table 2 are chosen to absorb the one-loop divergences in the amplitudes [12, 13, 14]. The scale dependences of the coupling constants and of the loop amplitude cancel in any physical quantity. The final amplitudes of  $O(p^4)$  are finite and scale independent.

The renormalized coupling constants  $N_i^r(\mu)$  are measurable quantities. A crucial question is whether all the coupling constants  $N_i$  corresponding to the operators  $W_i$  in Table 2

| i  | $W_i$  | $Z_i$ |
|----|--|-------|
| 14 | $i\langle\lambda\{F_L^{\mu\nu} + U^\dagger F_R^{\mu\nu} U, D_\mu U^\dagger D_\nu U\}\rangle$   | 1/4   |
| 15 | $i\langle\lambda D_\mu U^\dagger (U F_L^{\mu\nu} U^\dagger + F_R^{\mu\nu}) D_\nu U\rangle$   | 1/2   |
| 16 | $i\langle\lambda\{F_L^{\mu\nu} - U^\dagger F_R^{\mu\nu} U, D_\mu U^\dagger D_\nu U\}\rangle$   | -1/4  |
| 17 | $i\langle\lambda D_\mu U^\dagger (U F_L^{\mu\nu} U^\dagger - F_R^{\mu\nu}) D_\nu U\rangle$   | 0     |
| 18 | $2\langle\lambda(F_L^{\mu\nu} U^\dagger F_{R\mu\nu} U + U^\dagger F_{R\mu\nu} U F_L^{\mu\nu})\rangle$                                | -1/8  |
| 28 | $i\varepsilon_{\mu\nu\rho\sigma}\langle\lambda D^\mu U^\dagger U\rangle\langle U^\dagger D^\nu U D^\rho U^\dagger D^\sigma U\rangle$ | 0     |
| 29 | $2\langle\lambda[U^\dagger \tilde{F}_R^{\mu\nu} U, D_\mu U^\dagger D_\nu U]\rangle$  | 0     |
| 30 | $\langle\lambda U^\dagger D_\mu U\rangle\langle(\tilde{F}_L^{\mu\nu} + U^\dagger \tilde{F}_R^{\mu\nu} U) D_\nu U^\dagger U\rangle$   | 0     |
| 31 | $\langle\lambda U^\dagger D_\mu U\rangle\langle(\tilde{F}_L^{\mu\nu} - U^\dagger \tilde{F}_R^{\mu\nu} U) D_\nu U^\dagger U\rangle$   | 0     |

Table 2: The octet operators  $W_i$  of the  $O(p^4)$  weak chiral Lagrangian (1.9) relevant for non-leptonic radiative  $K$  decays, together with the corresponding renormalization constants  $Z_i$ . The dual field strength tensors are denoted as  $\tilde{F}_{L,R}^{\mu\nu}$ . Otherwise, the notation is the same as in [4].

can be measured in radiative  $K$  decay experiments. We list in Table 3 all the non-leptonic radiative transitions to which the  $N_i$  contribute. There are other decays not sensitive to the  $N_i$  that are either given by finite one-loop amplitudes and/or anomalous contributions at  $O(p^4)$  ( $K_S \rightarrow \gamma^* \gamma^*$ ,  $K^0 \rightarrow \pi^0 \gamma \gamma$ ,  $K^0 \rightarrow \pi^0 \pi^0 \gamma \gamma$ ,  $K_L \rightarrow \pi^+ \pi^- \gamma [\gamma]$ ) or which vanish even at  $O(p^4)$  ( $K_L \rightarrow \gamma^* \gamma^*$ ,  $K^0 \rightarrow \pi^0 \pi^0 \gamma$ ).

The information contained in Table 3 leads to the following conclusions:

- Read horizontally, one finds all parameter-free relations between radiative amplitudes of  $O(p^4)$ . If in the last column the renormalized constants  $N_i^r$  are displayed, the corresponding decays have divergent one-loop amplitudes. The other modes have finite loop amplitudes.
- Read vertically, we infer that from decays with at most two pions in the final state only the following combinations of counterterm coupling constants can in principle be extracted:

$$N_{14}, N_{15}, N_{16} + N_{17}, N_{18}, N_{29} + N_{31}, 3N_{29} - N_{30} . \quad (1.11)$$

Experiments at DAΦNE are expected to measure most of those decays.

- Decays with three pions in the final state are needed to determine  $N_{16}$  and  $N_{17}$  separately and the combination  $3N_{28} - 2N_{30}$ .
- Whereas all “electric” constants  $N_{14}, \dots, N_{18}$  can in principle be determined phenomenologically, this is not the case for the “magnetic” constants (the corresponding

| $\pi$               | $2\pi$                       | $3\pi$                      | $N_i$   |
|---------------------|------------------------------|-----------------------------|---|
| $\pi^+\gamma^*$     |                              |                             | $N_{14}^r - N_{15}^r$                             |
| $\pi^0\gamma^* (S)$ | $\pi^0\pi^0\gamma^* (L)$     |                             | $2N_{14}^r + N_{15}^r$                            |
| $\pi^+\gamma\gamma$ | $\pi^+\pi^0\gamma\gamma$     |                             | $N_{14} - N_{15} - 2N_{18}$                       |
|                     | $\pi^+\pi^-\gamma\gamma (S)$ |                             | "   |
|                     | $\pi^+\pi^0\gamma$           | $\pi^+\pi^+\pi^-\gamma$     | $N_{14} - N_{15} - N_{16} - N_{17}$               |
|                     | $\pi^+\pi^-\gamma (S)$       | $\pi^+\pi^0\pi^0\gamma$     | "   |
|                     |                              | $\pi^+\pi^-\pi^0\gamma (L)$ | "   |
|                     |                              | $\pi^+\pi^-\pi^0\gamma (S)$ | $7(N_{14}^r - N_{16}^r) + 5(N_{15}^r + N_{17}^r)$ |
|                     | $\pi^+\pi^-\gamma (L)$       | $\pi^+\pi^-\pi^0\gamma (S)$ | $N_{29} + N_{31}$                                 |
|                     |                              | $\pi^+\pi^+\pi^-\gamma$     | "   |
|                     | $\pi^+\pi^0\gamma$           | $\pi^+\pi^0\pi^0\gamma$     | $3N_{29} - N_{30}$                                |
|                     |                              | $\pi^+\pi^-\pi^0\gamma (S)$ | $2(N_{29} + N_{31}) + 3N_{29} - N_{30}$           |
|                     |                              | $\pi^+\pi^-\pi^0\gamma (L)$ | $6N_{28} - 4N_{30} + 3N_{29} - N_{30}$            |

Table 3: Decay modes to which the coupling constants  $N_i$  contribute. For the  $3\pi$  final states, only the single photon channels are listed. For the neutral modes, the letters  $L$  or  $S$  in brackets distinguish between  $K_L$  and  $K_S$  initial states in the limit of CP conservation.

operators  $W_i$  contain an  $\varepsilon$  tensor): only three combinations of the four constants  $N_{28}, \dots, N_{31}$  appear in measurable amplitudes.

Except for the radiative decays with three pions in the final state [11], all amplitudes appearing in Table 3 have been fully calculated to  $O(p^4)$ . Since DAΦNE will probably only be able to measure the lowest-order bremsstrahlung contributions for decays of the type  $K \rightarrow 3\pi\gamma$ , but not the interesting  $O(p^4)$  parts, the phenomenological determination of the  $N_i$  will remain incomplete. Nevertheless, the information expected from DAΦNE will be extremely valuable both for checking the parameter-free low-energy theorems of  $O(p^4)$  between different amplitudes and for testing the predictions of various models for the coupling constants  $N_i$  [13, 15, 16, 17, 18].

For non-leptonic  $K$  decays, the relevant expansion parameter for the chiral expansion of amplitudes is

$$\frac{M_K^2}{(4\pi F_\pi)^2} = 0.18 . \quad (1.12)$$

Although this expansion parameter is reasonably small, higher-order corrections beyond  $O(p^4)$  may in some cases be sizable. There is at this time no complete investigation of such higher-order effects even in the strong sector, not to speak of the non-leptonic weak sector. Some exploratory studies have already been performed and we shall come back to them in the subsequent sections. Already now, we want to emphasize that those investigations



should be viewed as attempts to locate the dominant higher-order effects rather than predictions of the same theoretical quality as the leading  $O(p^4)$  amplitudes.

### 1.3 The chiral anomaly in the non-leptonic weak sector

The contributions of the chiral anomaly to strong, electromagnetic and semileptonic weak amplitudes can be expressed in terms of the Wess–Zumino–Witten (WZW) functional [19]  $Z[U, l, r]_{\text{WZW}}$ . Its explicit form can be found in Ref. [4]. However, the chiral anomaly also contributes to non-leptonic weak amplitudes starting at  $O(p^4)$ . Two different manifestations of the anomaly can be distinguished.

The reducible anomalous amplitudes [9, 10] (type iii in the classification of Sect. 1.2) arise from the contraction of meson lines between a weak  $\Delta S = 1$  Green function and the WZW functional. At  $O(p^4)$ , there can only be one such contraction and the weak vertex must be due to the lowest-order non-leptonic Lagrangian  $\mathcal{L}_2^{\Delta S=1}$  in Eq. (1.4). Since  $\mathcal{L}_2^{\Delta S=1}$  contains bilinear terms in the meson fields, the so-called pole contributions to anomalous non-leptonic amplitudes can be given in closed form by a simultaneous diagonalization [6, 7] of the kinetic parts of the Lagrangians  $\mathcal{L}_2$  and  $\mathcal{L}_2^{\Delta S=1}$ . The corresponding local Lagrangian (octet part only) is [9, 10]:

$$\mathcal{L}_{\text{an}}^{\Delta S=1} = \frac{ieG_8}{8\pi^2 F} \tilde{F}^{\mu\nu} \partial_\mu \pi^0 K^+ \overleftrightarrow{D}_\nu \pi^- + \frac{\alpha G_8}{6\pi F} \tilde{F}^{\mu\nu} F_{\mu\nu} \left( K^+ \pi^- \pi^0 - \frac{1}{\sqrt{2}} K^0 \pi^+ \pi^- \right) + \text{h.c.} \quad (1.13)$$

Here  $F_{\mu\nu} = \partial_\mu A_\nu - \partial_\nu A_\mu$  is the electromagnetic field strength tensor,  $\tilde{F}_{\mu\nu} = \varepsilon_{\mu\nu\rho\sigma} F^{\rho\sigma}$  its dual and  $D_\mu \varphi^\pm = (\partial_\mu \pm ieA_\mu) \varphi^\pm$  denotes the covariant derivative with respect to electromagnetism.

There are also other reducible anomalous amplitudes. A generic example is provided by a non-leptonic Green function where an external  $\pi^0$  or  $\eta$  makes an anomalous transition to two photons. Such transitions are the dominant  $O(p^4)$  contributions to the decays  $K_S \rightarrow \pi^0 \gamma \gamma$  [6] and  $K_L \rightarrow \pi^0 \pi^0 \gamma \gamma$  [20, 21]. All reducible anomalous amplitudes of  $O(p^4)$  are proportional to  $G_8$  in the octet limit. No other unknown parameters are involved.

The second manifestation of the anomaly in non-leptonic weak amplitudes arises diagrammatically from the contraction of the  $W$  boson field between a strong Green function on one side and the WZW functional on the other side. However, such diagrams cannot be taken literally at a typical hadronic scale because of the presence of strongly interacting fields on both sides of the  $W$ . Instead, one must first integrate out the  $W$  together with the heavy quark fields. The operators appearing in the operator product expansion must then be realized at the bosonic level in the presence of the anomaly.

Following the methods of Ref. [22], the bosonization of four-quark operators in the odd-intrinsic parity sector was investigated in Ref. [18]. As in the even-intrinsic parity sector, the bosonized four-quark operators contain factorizable (leading in  $1/N_c$ , where  $N_c$  is the number of colours) and non-factorizable parts (non-leading in  $1/N_c$ ). Due to the non-renormalization theorem [23] of the chiral anomaly, the factorizable contributions of  $O(p^4)$

| Transition   | $\mathcal{L}_{\text{an}}^{\Delta S=1}$ | $W_{28}$ | $W_{29}$ | $W_{30}$ | $W_{31}$ | expt. |
|--|--|----------|----------|----------|----------|-------|
| $K^+ \rightarrow \pi^+ \pi^0 \gamma$               | x                                      |          | x        | x        |          | x     |
| $K^+ \rightarrow \pi^+ \pi^0 \gamma \gamma$        | x                                      |          | x        | x        |          |       |
| $K_L \rightarrow \pi^+ \pi^- \gamma$               |  |          | x        |          | x        | x     |
| $K_L \rightarrow \pi^+ \pi^- \gamma \gamma$        | x                                      |          | x        |          | x        |       |
| $K^+ \rightarrow \pi^+ \pi^0 \pi^0 \gamma$         |  |          | x        | x        |          | x     |
| $K^+ \rightarrow \pi^+ \pi^0 \pi^0 \gamma \gamma$  |  |          | x        | x        |          |       |
| $K^+ \rightarrow \pi^+ \pi^+ \pi^- \gamma$         |  |          | x        |          | x        | x     |
| $K^+ \rightarrow \pi^+ \pi^+ \pi^- \gamma \gamma$  |  |          | x        |          | x        |       |
| $K_L \rightarrow \pi^+ \pi^- \pi^0 \gamma$         |  | x        | x        | x        |          |       |
| $K_S \rightarrow \pi^+ \pi^- \pi^0 \gamma(\gamma)$ |  |          | x        | x        | x        |       |

Table 4: A complete list of local anomalous non-leptonic weak  $K$  decay amplitudes of  $O(p^4)$  in the limit of CP conservation.

can be calculated exactly [18]. It turns out that the factorizable contributions produce all the relevant octet operators proportional to the  $\varepsilon$  tensor ( $W_{28}$ ,  $W_{29}$ ,  $W_{30}$  and  $W_{31}$  in Table 2). The non-factorizable parts automatically have the right octet transformation property (they do not get any contribution from the anomaly) and are therefore also of the form  $W_{28}, \dots, W_{31}$ . Altogether, the  $\Delta S = 1$  effective Lagrangian in the anomalous parity sector of  $O(p^4)$  can be characterized by the coefficients [18]

$$\begin{aligned}
N_{28}^{\text{an}} &= \frac{a_1}{8\pi^2} & N_{29}^{\text{an}} &= \frac{a_2}{32\pi^2} \\
N_{30}^{\text{an}} &= \frac{3a_3}{16\pi^2} & N_{31}^{\text{an}} &= \frac{a_4}{16\pi^2},
\end{aligned} \tag{1.14}$$

where the dimensionless coefficients  $a_i$  are expected to be positive and of order one (most probably smaller than one [18]).

In Table 4 we list all kinematically allowed non-leptonic  $K$  decays that are sensitive either to the anomalous Lagrangian  $\mathcal{L}_{\text{an}}^{\Delta S=1}$  in (1.13) or to the direct terms of  $O(p^4)$  via (1.14). A separate column indicates whether the corresponding decay has been observed experimentally. The transitions with either three pions and/or two photons in the final state are in general also subject to non-local reducible anomalous contributions. In the non-leptonic weak sector, the chiral anomaly contributes only to *radiative*  $K$  decays.

## 2 Kaon decays with two photons in the final state

Two photons can have either  $CP = +1$  or  $CP = -1$ . Thus in the case of only two photons in the final state, due to gauge invariance, the amplitude will be proportional either to

$F_{\mu\nu}F^{\mu\nu}$  (parallel polarization,  $CP = +1$ ) or to  $\varepsilon_{\mu\nu\rho\lambda}F^{\mu\nu}F^{\rho\lambda}$  (perpendicular polarization,  $CP = -1$ ). In the case of one or more pions in the final state also other invariant amplitudes will appear.

## 2.1 $K_S \rightarrow \gamma\gamma$

We will consider the CP conserving amplitude  $A(K_S \rightarrow \gamma\gamma)$  in the framework of CHPT [24]. Since  $K^0$  is neutral, there is no tree level contribution to  $K^0 \rightarrow \gamma\gamma$ . At  $O(p^4)$ , there are in principle both chiral meson loops (Fig. 1) and  $O(p^4)$  counterterms. Again because of  $K^0$  being neutral,  $O(p^4)$  counterterms do not contribute. This has two implications:

- 1) the chiral meson loops are finite;
- 2) these are the only contributions of  $O(p^4)$  and there is no dependence on unknown coupling constants.

The finiteness of the one-loop amplitude can be simply understood by the fact that the superficial degree of divergence of the amplitude ( $\sim \Lambda^2$ , with  $\Lambda$  an ultraviolet cut-off) is decreased by gauge invariance together with the condition that the amplitude must vanish in the  $SU(3)$  limit. Thus the pion loop amplitude is proportional to  $A(K_1^0 \rightarrow \pi^+\pi^-)$ , i.e. to  $M_{K^0}^2 - M_{\pi^+}^2$ , while the kaon loop amplitude is proportional to  $M_{K^0}^2 - M_{K^+}^2$  and thus can be neglected.

Adding the 8- and 27-plet contributions one obtains [24, 25]

$$A(K_1^0 \rightarrow 2\gamma_{||}) = \frac{4\alpha F}{\pi M_K^2} (G_8 + \frac{2}{3}G_{27})(M_K^2 - M_\pi^2)[(q_1\epsilon_2)(q_2\epsilon_1) - (\epsilon_1\epsilon_2)(q_1q_2)]H(0), \quad (2.1)$$

where  $q_1, \epsilon_1, q_2, \epsilon_2$  are the photon momenta and polarizations. The function  $H$ , defined in App. A, has an imaginary part since the two pions can be on-shell.

The rate is given by

$$\Gamma(K_S \rightarrow 2\gamma_{||}) = \frac{(G_8 + \frac{2}{3}G_{27})^2(M_K^2 - M_\pi^2)^2\alpha^2 F^2}{4\pi^3 M_K} \cdot |H(0)|^2, \quad (2.2)$$

which implies  $\Gamma(K_S \rightarrow \gamma\gamma) = 1.5 \cdot 10^{-11} \text{eV}$ . The branching ratio is

$$BR(K_S \rightarrow \gamma\gamma) = 2.1 \cdot 10^{-6}, \quad (2.3)$$

corresponding to

$$\frac{\Gamma(K_S \rightarrow 2\gamma)_{theor}}{\Gamma(K_L \rightarrow 2\gamma)_{exp}} \approx 2. \quad (2.4)$$

The experimental branching ratio [26]

$$BR(K_S \rightarrow 2\gamma) = (2.4 \pm 1.2) \cdot 10^{-6} \quad (2.5)$$

is in good agreement with the prediction (2.3). This is a significant test for CHPT, since Eq. (2.3) is unambiguously predicted to  $O(p^4)$  in terms of the  $O(p^2)$  couplings  $G_8$  and  $G_{27}$ .

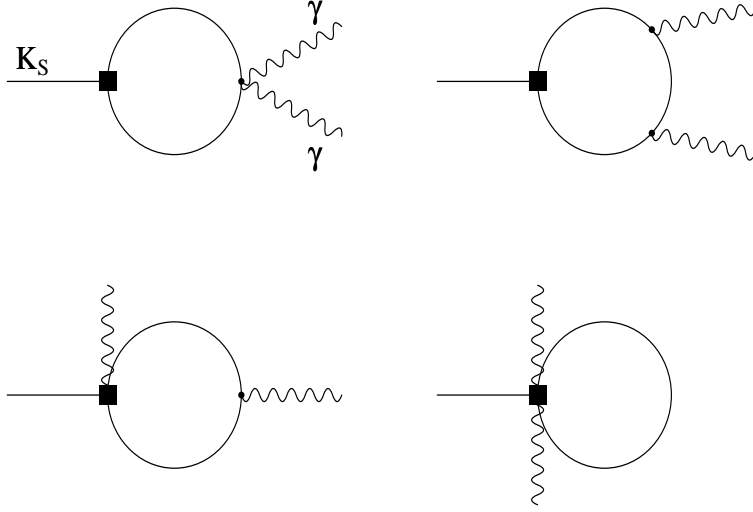


Figure 1: One-loop diagrams for  $K_S \rightarrow \gamma\gamma$ . The black squares indicate the weak vertices.

Indeed, the absence of  $O(p^4)$  counterterms not only implies that the amplitude is finite but it also ensures that contact terms will appear only at  $O(p^6)$  and are thus suppressed by the chiral expansion parameter  $M_K^2/(4\pi F_\pi)^2 \sim 0.2$ . This last statement is even more justified in this channel since there are no vector meson exchange contributions at this order. The effect of  $\pi - \pi$  rescattering has been shown to be negligible [27, 28]. Since the model independent absorptive part is dominant in this decay, one obtains similar results using a phenomenological coupling in the pion loop [29, 30].

## 2.2 $K_L \rightarrow \pi^0 \gamma\gamma$

The general amplitude for  $K_L \rightarrow \pi^0 \gamma\gamma$  is given by

$$M(K_L(p) \rightarrow \pi^0(p')\gamma(q_1, \varepsilon_1)\gamma(q_2, \varepsilon_2)) = \varepsilon_{1\mu}\varepsilon_{2\nu}M^{\mu\nu}(p, q_1, q_2) , \quad (2.6)$$

where  $\varepsilon_1, \varepsilon_2$  are the photon polarizations. If CP is conserved,  $M^{\mu\nu}$  can be decomposed in two invariant amplitudes:

$$\begin{aligned} M^{\mu\nu} = & \frac{A(y, z)}{M_K^2}(q_2^\mu q_1^\nu - q_1 \cdot q_2 g^{\mu\nu}) \\ & + \frac{2B(y, z)}{M_K^4}(-p \cdot q_1 p \cdot q_2 g^{\mu\nu} - q_1 \cdot q_2 p^\mu p^\nu + p \cdot q_1 q_2^\mu p^\nu + p \cdot q_2 p^\mu q_1^\nu) , \end{aligned} \quad (2.7)$$

with

$$y = p \cdot (q_1 - q_2)/M_K^2 , \quad z = (q_1 + q_2)^2/M_K^2 . \quad (2.8)$$

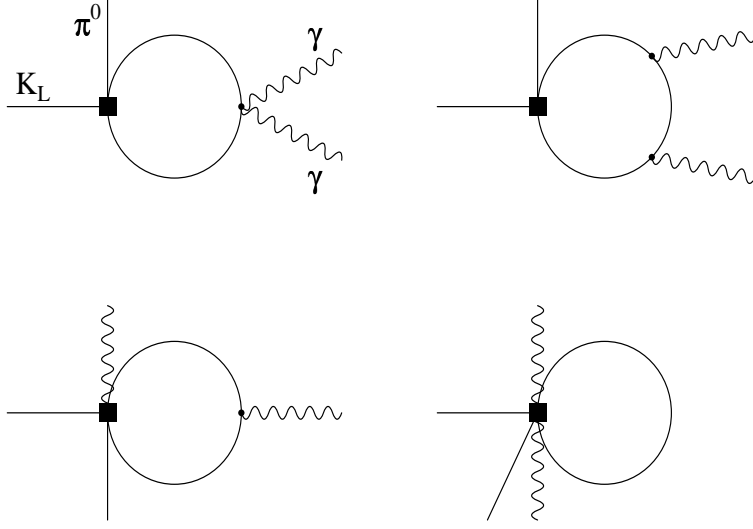


Figure 2: One-loop diagrams for  $K_L \rightarrow \pi^0 \gamma \gamma$  in the diagonal basis of Refs. [6, 7].

Due to Bose symmetry  $A(y, z)$  and  $B(y, z)$  must be symmetric for  $q_1 \leftrightarrow q_2$  and consequently depend only on  $y^2$ .

The physical region in the dimensionless variables  $y$  and  $z$  is given by the inequalities

$$|y| \leq \frac{1}{2} \lambda^{1/2}(1, z, r_\pi^2), \quad 0 \leq z \leq (1 - r_\pi)^2, \quad (2.9)$$

where  $r_\pi = M_\pi/M_K$  and the function  $\lambda$  is defined in App. A. From (2.6) and (2.7) we obtain the double differential decay rate for unpolarized photons:

$$\frac{d^2 \Gamma}{dy dz} = \frac{M_K}{2^9 \pi^3} \left\{ z^2 |A + B|^2 + \left[ y^2 - \frac{1}{4} \lambda(1, z, r_\pi^2) \right]^2 |B|^2 \right\}. \quad (2.10)$$

We remark that, due to the different tensor structure in (2.7), the  $A$  and  $B$  parts of the amplitude give rise to contributions to the differential decay rate which have different dependence on the two-photon invariant mass  $z$ . In particular, the second term in (2.10) gives a non-vanishing contribution to  $\frac{d\Gamma(K_L \rightarrow \pi^0 \gamma \gamma)}{dz}$  in the limit  $z \rightarrow 0$ . Thus the kinematical region with collinear photons is important to extract the  $B$  amplitude.

We now consider this decay in the framework of CHPT. Since  $K_L$  and  $\pi^0$  are neutral there is no tree level  $O(p^2)$  contribution. At  $O(p^4)$ , there are in principle both loops and counterterms. Since again  $K_L$  and  $\pi^0$  are neutral the latter ones do not contribute implying a finite one-loop amplitude [6, 31]. The relevant diagrams are shown in Fig. 2. At  $O(p^4)$ , the amplitude  $B$  vanishes because there are not enough powers of momenta. The result for the amplitude  $A$  (which at this order depends only on  $z$ ) due to the octet piece of the

non-leptonic weak Lagrangian is [6, 31]:

$$A^{(8)}(z) = \frac{G_8 \alpha M_K^2}{\pi} \left[ \left(1 - \frac{r_\pi^2}{z}\right) \cdot F\left(\frac{z}{r_\pi^2}\right) - \left(1 - \frac{r_\pi^2}{z} - \frac{1}{z}\right) F(z) \right] . \quad (2.11)$$

The function  $F(z)$ , defined in App. A, is real for  $z \leq 4$  and complex for  $z \geq 4$ . In (2.11), the contribution proportional to  $F(z)$ , which does not have an absorptive part, comes from the kaon loop, while the one proportional to  $F(\frac{z}{r_\pi^2})$ , generated by the pion loop, has an absorptive part since the pions can be on-shell. Consequently, the kaon loop contribution is much smaller than the pion one. For completeness we mention the contribution of the  $(27_L, 1_R)$  operator. Due to the vanishing of the corresponding counterterms also this contribution is finite and unambiguously predicted. For the pion loop, which gives the larger contribution, one obtains [32]:

$$A_{1/2}^{(27)}(z) = \frac{G_{27} \alpha M_K^2}{9\pi} \left(1 - \frac{r_\pi^2}{z}\right) F\left(\frac{z}{r_\pi^2}\right) \quad (2.12)$$

$$A_{3/2}^{(27)}(z) = -\frac{5G_{27} \alpha M_K^2}{18\pi} \left[ \frac{3 - r_\pi^2 - 14r_\pi^4 - (5 - 14r_\pi^2)z}{(1 - r_\pi^2)z} \right] F\left(\frac{z}{r_\pi^2}\right) . \quad (2.13)$$

Compared to the octet, there is a slight modification of the spectrum and of the width.

The  $z$  spectrum for a  $y$ -independent amplitude  $A$  is given by:

$$\frac{d\Gamma}{dz} = \frac{M_K}{2^{10}\pi^3} z^2 \lambda^{1/2}(1, z, r_\pi^2) |A(z)|^2 . \quad (2.14)$$

The  $O(p^4)$  CHPT prediction for  $\frac{d\Gamma}{dz}(K_L \rightarrow \pi^0 \gamma \gamma)$  is shown in Fig. 3, while the prediction for the branching ratio is:

$$BR^{(8)}(K_L \rightarrow \pi^0 \gamma \gamma) = 6.8 \cdot 10^{-7}, \quad BR^{(8+27)}(K_L \rightarrow \pi^0 \gamma \gamma) = 6.0 \cdot 10^{-7} . \quad (2.15)$$

The spectrum predicted by CHPT to  $O(p^4)$  is very characteristic: a peak in the absorptive region ( $K_L \rightarrow \pi \pi \pi \rightarrow \pi \gamma \gamma$ ) and a negligible contribution at low  $z$ . As we shall see, contrary to the  $K_S \rightarrow \gamma \gamma$  case, corrections to the  $O(p^4)$  CHPT prediction for  $K_L \rightarrow \pi^0 \gamma \gamma$  can be sizable [15]. Phenomenological models with large vector or scalar exchange [33, 34, 35, 36, 37] can generate a larger branching ratio. However, due to the presence of a  $B$  amplitude, a non-vanishing contribution to the spectrum at low  $z$  is in general expected in such models.

Another point of interest of  $K_L \rightarrow \pi^0 \gamma \gamma$  is its role as an intermediate state in  $K_L \rightarrow \pi^0 e^+ e^-$ . The decay  $K_L \rightarrow \pi^0 e^+ e^-$  has three kinds of contributions [1, 38, 15, 39, 40]: direct CP violation, indirect CP violation via  $K^0 - \bar{K}^0$  mixing (cf.  $K_S \rightarrow \pi^0 e^+ e^-$  in Sect. 4) and the CP conserving transition  $K_L \rightarrow \pi^0 \gamma^* \gamma^* \rightarrow \pi^0 e^+ e^-$ . The direct CP violating contribution is expected to give  $BR(K_L \rightarrow \pi^0 e^+ e^-) \simeq 10^{-11}$  [41]. At  $O(p^4)$ , the

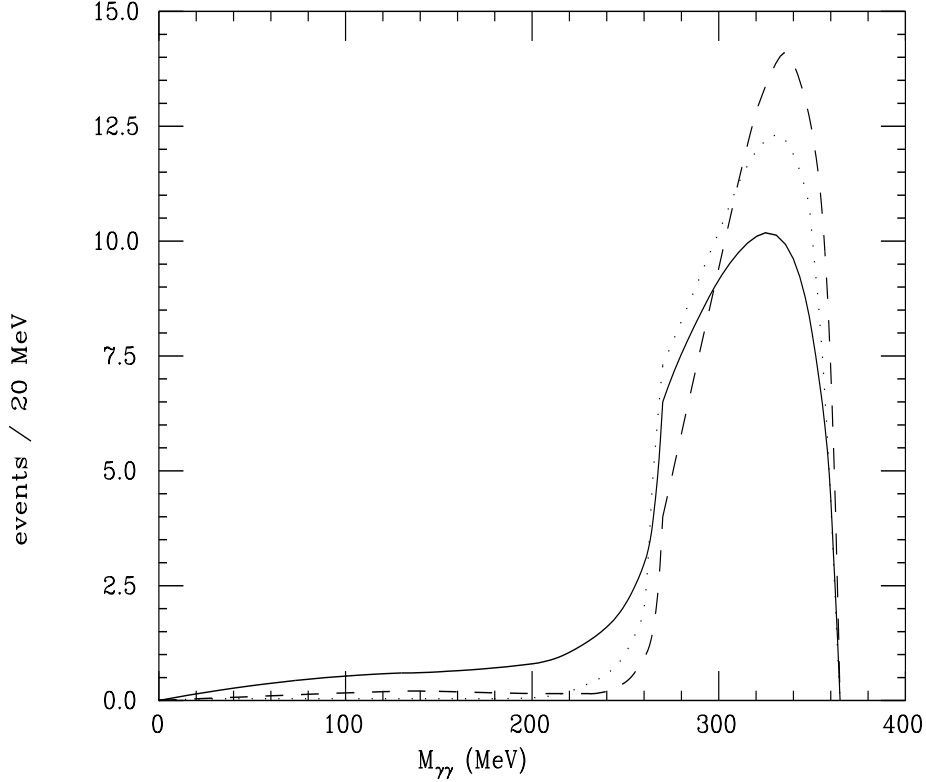


Figure 3: Theoretical predictions for the  $2\gamma$  invariant mass distribution in  $K_L \rightarrow \pi^0 \gamma \gamma$ . The dotted curve is the  $O(p^4)$  contribution, the dashed and full curves correspond to the  $O(p^6)$  calculation of [45] with  $a_V = 0$  and  $a_V = -0.9$ , respectively. The spectra are normalized to the 50 unambiguous events of NA31 (cf. Fig. 4).

contribution of  $K_L \rightarrow \pi^0 \gamma \gamma$  to this process is helicity suppressed via the amplitude  $A$ :  $BR(K_L \rightarrow \pi^0 e^+ e^-) \simeq 10^{-14}$ . However, at  $O(p^6)$  the amplitude  $B$  is generated. Although this amplitude is a higher-order effect in CHPT, the corresponding amplitude for  $K_L \rightarrow \pi^0 e^+ e^-$  is not helicity suppressed [7] and could be substantially larger than the leading-order contribution due to  $A$ . We stress again that the presence of a  $B$  amplitude could be checked experimentally by studying the spectrum of  $K_L \rightarrow \pi^0 \gamma \gamma$  at low  $z$ .

From the experimental point of view, an important background for this process is  $K_L \rightarrow \pi^0 \pi^0$ , which makes it difficult to explore the region  $z \sim \frac{M_\pi^2}{M_K^2}$ . The experimental situation is the following:

$$BR(K_L \rightarrow \pi^0 \gamma \gamma) = (1.7 \pm 0.2 \pm 0.2) \cdot 10^{-6} \text{ for } M_{\gamma\gamma} > 280 \text{ MeV NA31 [42],} \quad (2.16)$$

$$BR(K_L \rightarrow \pi^0 \gamma \gamma) = (1.86 \pm 0.60 \pm 0.60) \cdot 10^{-6} \text{ for } M_{\gamma\gamma} > 280 \text{ MeV E731 [43],} \quad (2.17)$$

where  $M_{\gamma\gamma}$  is the two-photon invariant mass:

$$M_{\gamma\gamma} = \sqrt{(q_1 + q_2)^2}. \quad (2.18)$$

In Fig. 4 the NA31 two-photon invariant mass histogram is displayed. We see that, although the rate seems underestimated, the number of events for  $M_{\gamma\gamma} < 240$  MeV is very small, as predicted by  $O(p^4)$  CHPT. There is no evidence for a sizable  $B$  term.

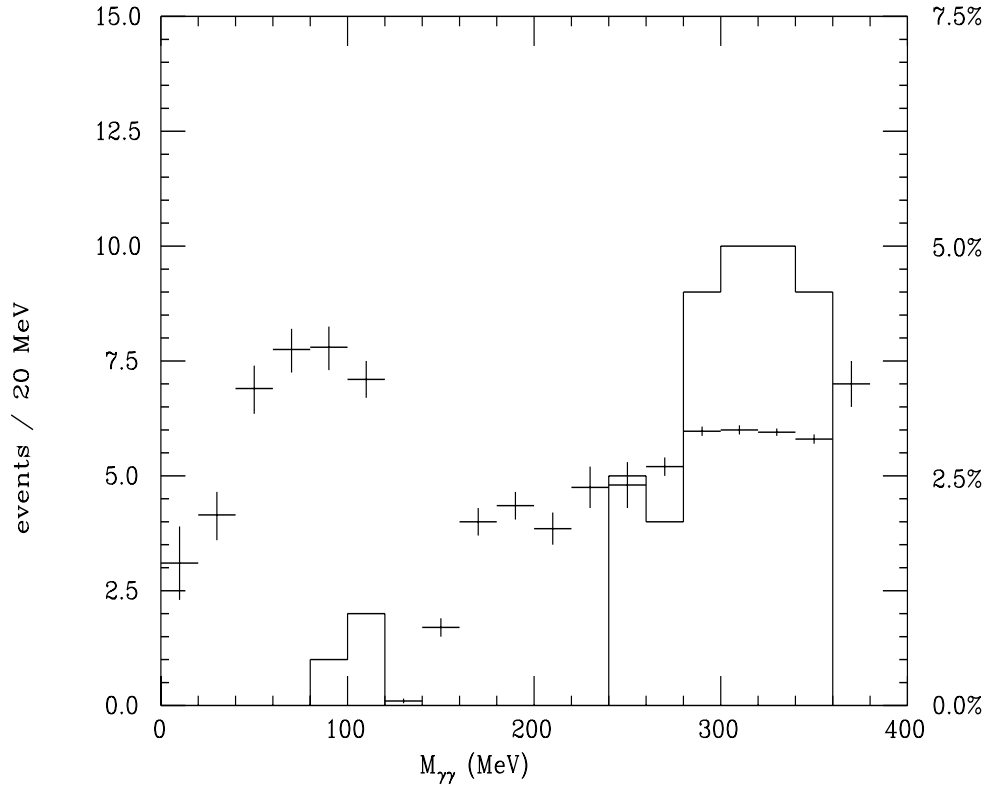


Figure 4:  $2\gamma$  invariant mass distribution for unambiguous  $K_L \rightarrow \pi^0\gamma\gamma$  candidates [42] (solid histogram). The crosses indicate the acceptance.

Several contributions have been analysed that go beyond  $O(p^4)$ .

The first and more controversial contributions are due to vector (and/or axial-vector and/or scalar) mesons. These can show up either in the weak couplings or in the strong ones. While model predictions for the strong couplings can be checked from experiments, this is not so easy for the weak ones. Some phenomenological models can generate large vector [34, 35, 36] or scalar exchange [37] contributions. One can parametrize the local  $O(p^6)$  contributions to  $K_L \rightarrow \pi^0\gamma\gamma$ , including direct weak transitions, by an effective vector coupling  $a_V$  [15] :

$$A = \frac{G_8 M_K^2 \alpha}{\pi} a_V (3 - z + r_\pi^2) , \quad B = -\frac{2G_8 M_K^2 \alpha}{\pi} a_V . \quad (2.19)$$

Thus,  $V$  exchange generates a  $B$  amplitude changing the  $O(p^4)$  spectrum, particularly in the region of small  $z$ , and contributing to the CP conserving part of  $K_L \rightarrow \pi^0 e^+ e^-$ . The  $B$  amplitude gives rise to

$$BR(K_L \rightarrow \pi^0 e^+ e^-)|_{abs} = 4.4 \cdot 10^{-12} a_V^2 . \quad (2.20)$$

From the analysis of events with  $M_{\gamma\gamma} < 240$  MeV, NA31 [42] have obtained the following limits:

$$-0.32 < a_V < 0.19 \quad (90\% \text{ CL}). \quad (2.21)$$



However, other  $O(p^6)$  contributions have to be included [44]. Since  $G_8$  appearing in (2.11) has been extracted from  $K_S \rightarrow 2\pi$  underestimating the  $K_L \rightarrow 3\pi$  amplitudes by 20% ÷ 30%, the authors of [32, 45] included the  $O(p^4)$  corrections to  $K_L \rightarrow 3\pi$  for the weak vertex in Fig. 2. The main feature of the analysis of [32, 45] is an increase of the width by some 25% and a modification of the spectrum. In fact, the resulting spectrum is even more strongly peaked at large  $z$  than found experimentally (see Fig. 3). However, the contribution of vector mesons in (2.19) still has to be added. Choosing  $a_V$  to reproduce the experimental spectrum leads to an additional increase of the rate [45] in good agreement with the measured values (2.16), (2.17). The corresponding contribution to  $K_L \rightarrow \pi^0 e^+ e^-$  ( $2\gamma$  absorptive part only) is still smaller than the direct CP violating contribution [45]. Finally, a more complete unitarization of the  $\pi - \pi$  intermediate states (Khuri–Treiman treatment) and the inclusion of the experimental  $\gamma\gamma \rightarrow \pi^0 \pi^0$  amplitude increases the  $K_L \rightarrow \pi^0 \gamma\gamma$  width by another 10% [27].

DAΦNE seems an ideal machine to investigate the relative role of CHPT and VMD in  $K_L \rightarrow \pi^0 \gamma\gamma$ , establishing both the absorptive and the dispersive part of the decay amplitude. In particular, the region of collinear photons could be definitely assessed.

### 2.3 $K_L \rightarrow \gamma\gamma$

If CP is conserved,  $K_L$  decays into two photons with perpendicular polarizations ( $2\gamma_\perp$ ). DAΦNE could improve the measurement of the decay width. However, since the theory for this channel is afflicted by several uncertainties, it will be difficult to achieve new insight from this measurement alone. This decay has been historically very important to understand the GIM mechanism [46]. The interplay between the short–distance contributions in Fig. 5 and the long–distance contribution in Fig. 6 is a matter of past and current interest [47, 48, 30]. This is also related to the study of CP violation in this channel at LEAR [49, 29, 25, 30, 50]. The experimental width  $\Gamma(K_L \rightarrow \gamma\gamma)$  is needed to predict direct CP violation in this channel. More generally, it will be useful for the theoretical analysis of other decays (cf. Sect. 4).

The loop integral of the short–distance contribution in Fig. 5 is a function of  $m_i^2/M_W^2$ , where  $m_i$  is the mass of the intermediate quark. The contributions for  $m_i = 0$  cancel when we sum over all  $u$ –like quarks (GIM mechanism). Also for  $m_i \neq 0$  the short–distance contributions are negligible compared to the long–distance ones [46, 47]. Thus, the main contribution is expected to come from long distances. In the framework of CHPT, the Wess–Zumino term and the  $\Delta S = 1$  weak Lagrangian generate the CP conserving amplitude. At  $O(p^4)$  in CHPT one has:

$$\begin{aligned} A(K_L \rightarrow 2\gamma_\perp)_{O(p^4)} &= A(K_L \rightarrow \pi^0 \rightarrow 2\gamma_\perp) + A(K_L \rightarrow \eta_8 \rightarrow 2\gamma_\perp) \\ &= A(K_L \rightarrow \pi^0)A(\pi^0 \rightarrow 2\gamma_\perp) \left[ \frac{1}{M_K^2 - M_\pi^2} + \frac{1}{3} \cdot \frac{1}{M_K^2 - M_8^2} \right] \simeq 0 . \end{aligned} \quad (2.22)$$

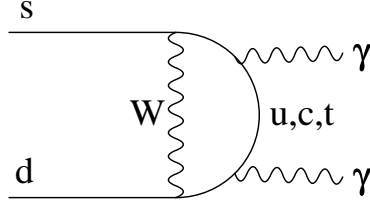


Figure 5: Short-distance contribution to  $K_L \rightarrow \gamma\gamma$ .

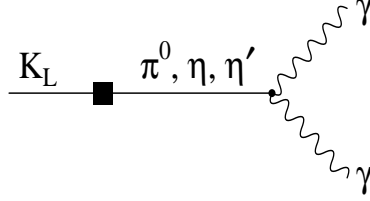


Figure 6: Long-distance contribution to  $K_L \rightarrow \gamma\gamma$ .

The Gell-Mann–Okubo formula, which holds at this order, tells us that the amplitude (2.22) is zero at  $O(p^4)$ . If we write the full amplitude as

$$A(K_L \rightarrow 2\gamma_\perp) = A(K_L \rightarrow \pi^0)A(\pi^0 \rightarrow 2\gamma_\perp)\frac{F_2}{M_K^2}, \quad (2.23)$$

one would naively expect  $F_2 \sim M_K^2/(4\pi F)^2 \simeq 0.2$ . However, comparison with experiment shows that  $F_2^{(exp)} \simeq 0.9$  implying large higher-order corrections in CHPT. At  $O(p^6)$ , the  $\eta'$  pole appears and contributes to the large value of  $F_2^{(exp)}$ . The pole contributions to the amplitude can be written as [46, 47, 48, 24, 29, 51, 25]

$$A(K^0 \rightarrow 2\gamma_\perp) = \sum_{P=\pi^0, \eta, \eta'} \frac{A(K^0 \rightarrow P)}{M_K^2 - M_P^2} A(P \rightarrow 2\gamma_\perp). \quad (2.24)$$

Including the  $\eta - \eta'$  mixing angle  $\Theta$ ,  $F_2$  defined in (2.23) is given by

$$F_2 = \frac{1}{1 - r_\pi^2} - \frac{(c_\Theta - 2\sqrt{2}s_\Theta)(c_\Theta + 2\sqrt{2}\rho s_\Theta)}{3(r_\eta^2 - 1)} + \frac{(2\sqrt{2}c_\Theta + s_\Theta)(2\sqrt{2}\rho c_\Theta - s_\Theta)}{3(r_{\eta'}^2 - 1)} \quad (2.25)$$

$$r_i = M_i/M_K, \quad c_\Theta = \cos \Theta, \quad s_\Theta = \sin \Theta.$$

$\rho \neq 1$  takes into account possible deviations from nonet symmetry for the non-leptonic weak vertices (nonet symmetry is assumed for the strong WZW vertices). The  $1/N_c$  prediction  $\Theta \simeq -20^\circ$  [52] and nonet symmetry agree very well with the  $2\gamma$  decay widths of  $\pi^0, \eta, \eta'$  [53].

The  $\eta$  and  $\eta'$  contributions in (2.25) interfere destructively for  $0 \leq \rho < 1$  and  $\Theta \simeq -20^\circ$ .  $F_2$  is dominated by the pion pole (cf. the similar situation for  $K_L \rightarrow \pi^+\pi^-\gamma$  discussed in Sect. 3). Since there are certainly other contributions of  $O(p^6)$  and higher, Eq. (2.25) at best contains the dominant contributions.

## 2.4 $K^+ \rightarrow \pi^+\gamma\gamma$

At present there is only an upper bound for the branching ratio of this process [54], which depends upon the shape of the spectrum due to the different experimental acceptance:

$$BR(K^+ \rightarrow \pi^+\gamma\gamma)_{exp} \leq 1.5 \cdot 10^{-4} \quad \text{CHPT amplitude.} \quad (2.26)$$

$$BR(K^+ \rightarrow \pi^+\gamma\gamma)_{exp} \leq 1.0 \cdot 10^{-6} \quad \text{constant amplitude.} \quad (2.27)$$

A cut in the two-photon invariant mass is necessary to disentangle this channel from the background  $K^+ \rightarrow \pi^+\pi^0 \rightarrow \pi^+\gamma\gamma$ .

Gauge invariance and chiral symmetry imply that this decay starts at  $O(p^4)$  in CHPT [cf. Eq. (1.7)]. Two invariant amplitudes contribute at this order:

$$\begin{aligned} M(K^+(p) \rightarrow \pi^+(p')\gamma(q_1, \epsilon_1)\gamma(q_2, \epsilon_2)) = \\ = \epsilon_\mu(q_1)\epsilon_\nu(q_2) \left[ A(y, z) \frac{(q_2^\mu q_1^\nu - q_1 \cdot q_2 g^{\mu\nu})}{M_K^2} + C(y, z) \varepsilon^{\mu\nu\alpha\beta} \frac{q_{1\alpha} q_{2\beta}}{M_K^2} \right], \end{aligned} \quad (2.28)$$

where  $y, z$  have been defined in (2.8) and the physical region for  $y, z$  is given in (2.9). The amplitude  $A$  corresponds to a  $2\gamma$  state with  $CP = +1$ , while  $C$  corresponds to a state with  $CP = -1$ . Compared to (2.7), the new amplitude  $C(y, z)$  appears because initial and final states are not CP eigenstates. Since  $A$  and  $C$  depend only on  $z$  at  $O(p^4)$ , we integrate over  $y$  to obtain the following expression for the two-photon invariant mass spectrum:

$$\frac{d\Gamma}{dz}(K^+ \rightarrow \pi^+\gamma\gamma) = \frac{M_K}{2^{10}\pi^3} z^2 \lambda^{\frac{1}{2}}(1, z, r_\pi^2) (|A(z)|^2 + |C(z)|^2). \quad (2.29)$$

The calculation for this decay proceeds similarly to the case of  $K_L \rightarrow \pi^0\gamma\gamma$ . The crucial difference is that now the  $O(p^4)$  counterterms do not vanish since here the external kaon and pion are charged. Loops and counterterms contribute to  $A$ , while the reducible anomalous amplitude (cf. Sect. 1) of Fig. 7 contributes to  $C$ .

The loop contribution turns out to be finite so that the total counterterm contribution must be scale independent. One finds [7]

$$A(z) = \frac{G_8 M_K^2 \alpha}{2\pi z} \left[ (r_\pi^2 - 1 - z) F\left(\frac{z}{r_\pi^2}\right) + (1 - r_\pi^2 - z) F(z) + \hat{c}z \right], \quad (2.30)$$

$$C(z) = \frac{G_8 M_K^2 \alpha}{\pi} \left[ \frac{z - r_\pi^2}{z - r_\pi^2 + i r_\pi \frac{\Gamma_{\pi^0}}{M_K}} - \frac{z - \frac{2+r_\pi^2}{3}}{z - r_\eta^2} \right], \quad (2.31)$$

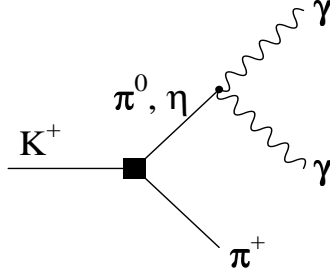


Figure 7: Pole diagram for  $K^+ \rightarrow \pi^+ \gamma \gamma$ .

where  $\hat{c}$  is an unknown coupling constant due to  $O(p^4)$  counterterms:

$$\hat{c} = \frac{128\pi^2}{3} [3(L_9 + L_{10}) + N_{14} - N_{15} - 2N_{18}] . \quad (2.32)$$

$L_9 + L_{10}$  and  $N_{14} - N_{15} - 2N_{18}$  are separately scale independent. In (2.30), the term proportional to  $F(z)$  comes from the kaon loop and does not have an absorptive part, while the term with  $F(\frac{z}{r_\pi^2})$  is due to the pion loop and has an absorptive part. As for  $K_L \rightarrow \pi^0 \gamma \gamma$ , the kaon loop contribution is much smaller than the pion loop one.

Using (2.30) and (2.31) in (2.29), one obtains

$$\Gamma_A(K^+ \rightarrow \pi^+ \gamma \gamma) = (2.80 + 0.87\hat{c} + 0.17\hat{c}^2) \cdot 10^{-20} \text{ MeV} \quad (2.33)$$

$$\Gamma_C(K^+ \rightarrow \pi^+ \gamma \gamma) = 0.26 \cdot 10^{-20} \text{ MeV} \quad (2.34)$$

showing the dominance of the loop over the anomalous contribution. Since  $\hat{c}$  is unknown we can deduce from (2.33) only a lower bound for the rate, which is obtained for  $\hat{c} = -2.6$ :

$$\Gamma(K^+ \rightarrow \pi^+ \gamma \gamma) = \Gamma_A + \Gamma_C \geq 2 \cdot 10^{-20} \text{ MeV}, \quad (2.35)$$

or equivalently

$$BR(K^+ \rightarrow \pi^+ \gamma \gamma) \geq 4 \cdot 10^{-7} . \quad (2.36)$$

The spectrum (2.29) is predicted up to the unknown parameter  $\hat{c}$ . Experiments can test the predicted shape and constrain the possible values of  $\hat{c}$ . The shape is in fact very sensitive to the value of  $\hat{c}$  (see Fig. 8). In the factorization model (cf. Ref. [13] and references therein) one obtains

$$\hat{c} = \frac{(4\pi F_\pi)^2}{M_\rho^2} (1 - 2k_f) = 2.3(1 - 2k_f) \quad (2.37)$$

where  $k_f = O(1)$  is a free parameter of the model. As a special case, the weak deformation model [15] has  $k_f = 1/2$  and  $\hat{c} = 0$  implying  $BR(K^+ \rightarrow \pi^+ \gamma \gamma) = 6 \cdot 10^{-7}$ . Naive factorization corresponds to  $k_f = 1$  and  $\hat{c} = -2.3$  with  $BR(K^+ \rightarrow \pi^+ \gamma \gamma) = 4 \cdot 10^{-7}$ .

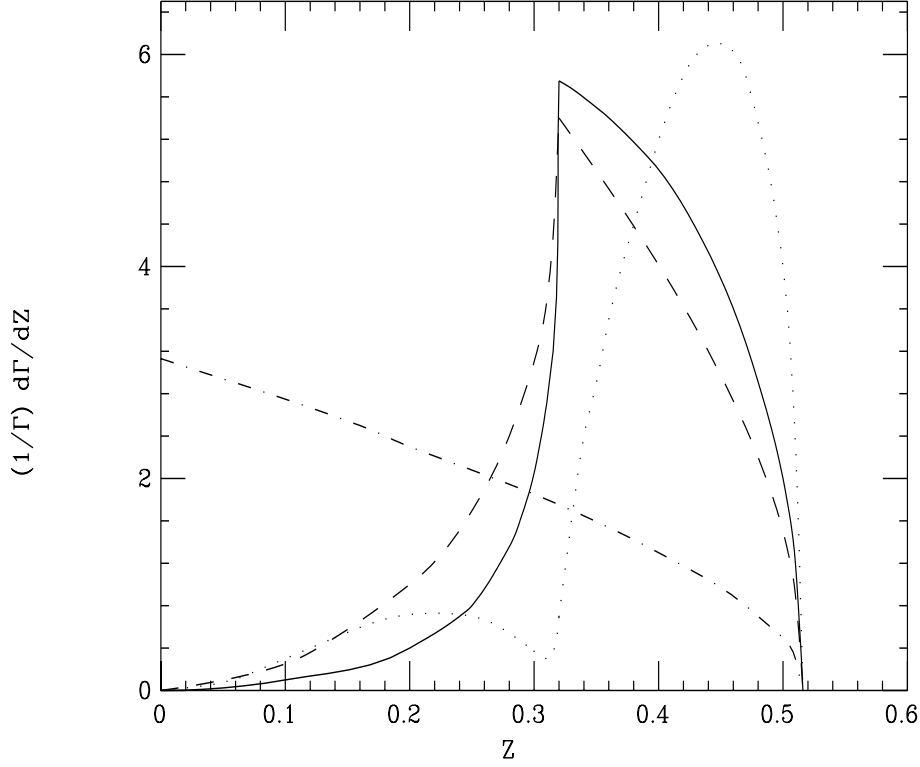


Figure 8: Normalized theoretical  $z$ -distribution in  $K^+ \rightarrow \pi^+ \gamma \gamma$  [7], for several values of  $\hat{c}$ :  $\hat{c} = 0$  (full curve),  $\hat{c} = 4$  (dashed curve) and  $\hat{c} = -4$  (dotted curve). The dash-dotted curve is the phase space.

## 2.5 $K_S \rightarrow \pi^0 \gamma \gamma$

This decay proceeds through a reducible anomalous amplitude similar to the one in Fig. 7, where  $K^+$  and  $\pi^+$  are replaced respectively by  $K_S$  and  $\pi^0$  [6]. We do not include  $\eta - \eta'$  mixing, which is a higher-order effect in CHPT. Actually, this process is mainly sensitive to the  $\pi^0$  pole, probing the momentum dependence of the  $K^0 \pi^0 \pi^0$  vertex. Due to the strong background coming from  $K_S \rightarrow \pi^0 \pi^0$ , a cut in  $z$  has to be applied.

The amplitude is given by [6]:

$$M(K_S(p) \rightarrow \pi^0(p') \gamma(q_1, \epsilon_1) \gamma(q_2, \epsilon_2)) = C(z) \varepsilon^{\mu\nu\alpha\beta} \frac{q_{1\alpha} q_{2\beta}}{M_K^2} \epsilon_\mu(q_1) \epsilon_\nu(q_2)$$

$$C(z) = \frac{G_8 \alpha M_K^2}{\pi} \left[ \frac{2 - z - r_\pi^2}{z - r_\pi^2 + i r_\pi \Gamma_{\pi^0} / M_K} - \frac{2 - 3z + r_\pi^2}{3(z - r_\eta^2 + i r_\eta \Gamma_\eta / M_K)} \right], \quad (2.38)$$

where  $r_i = \frac{M_i}{M_K}$ . The  $2\gamma$  invariant mass spectrum is dominated by the  $\pi^0$  pole and is given by

$$\frac{d\Gamma}{dz}(K_S \rightarrow \pi^0 \gamma \gamma) = \frac{M_K}{2^{10} \pi^3} z^2 \lambda^{\frac{1}{2}}(1, z, r_\pi^2) |C(z)|^2. \quad (2.39)$$

This spectrum and the one obtained with a constant weak coupling are shown in Fig. 9, where the cut  $z \geq 0.2$  has been applied. The branching ratio with this cut is

$$BR(K_S \rightarrow \pi^0 \gamma \gamma)_{z \geq 0.2} = 3.8 \cdot 10^{-8}. \quad (2.40)$$

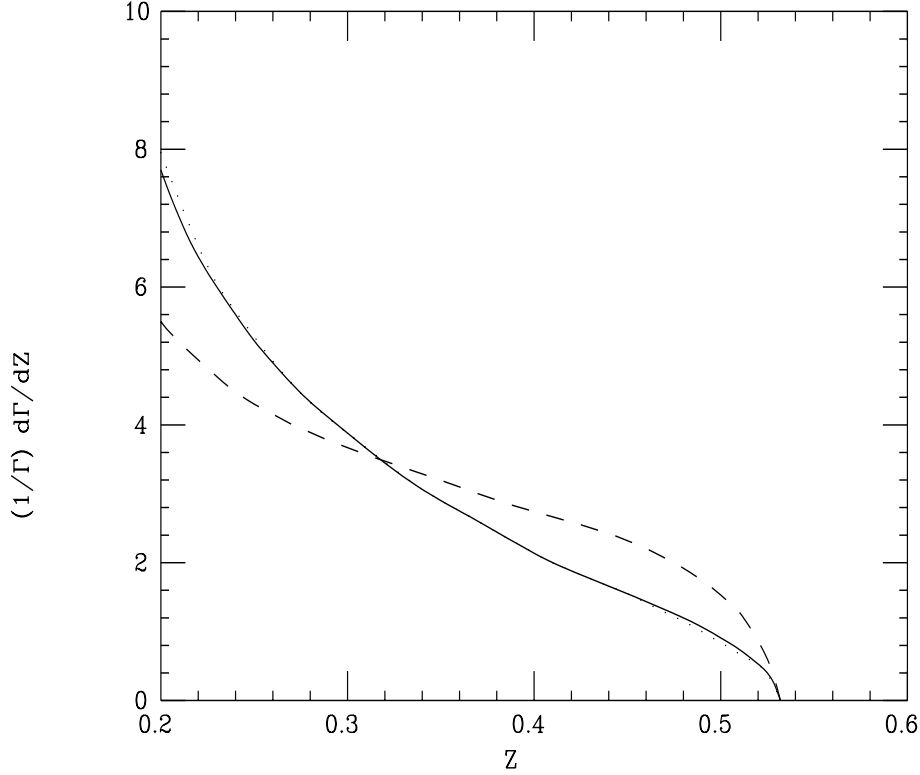


Figure 9: Normalized theoretical  $z$ -distribution in  $K_S \rightarrow \pi^0 \gamma \gamma$  [6] in the region  $0.2 \leq z \leq (1 - r_\pi)^2$  (full curve). The pion pole contribution alone is given by the dotted curve. The dashed curve is obtained assuming momentum independent weak vertices.

DAΦNE should be able to see this decay, but it will be very difficult to confirm the kinematical dependence of the vertex.

## 2.6 $K_{L,S} \rightarrow \pi^0 \pi^0 \gamma \gamma$

These decays can be unambiguously predicted in CHPT at  $O(p^4)$ . For both transitions there are no  $O(p^4)$  weak counterterms and thus the one-loop amplitude is finite.  $A(K_L \rightarrow \pi^0 \pi^0 \gamma \gamma)$  is a reducible anomalous amplitude [20], while  $A(K_S \rightarrow \pi^0 \pi^0 \gamma \gamma)$  is a pure loop amplitude [21].

From the experimental point of view, it is convenient for both decays to perform a cut in the two-photon invariant mass  $M_{\gamma\gamma}$  in order to avoid the background from  $K_{L,S} \rightarrow \pi^0 \pi^0 \pi^0$ ,  $K_{L,S} \rightarrow \pi^0 \pi^0$  and  $K_{L,S} \rightarrow \pi^0 \pi^0 \gamma$ . Following Ref. [21], we report in Table 5 the predictions for the two branching ratios, with cuts  $M_{\gamma\gamma} > \delta m$  and  $|M_{\gamma\gamma} - M_\pi| > \delta m$ , for different values of  $\delta m$ . Since  $K_L \rightarrow \pi^0 \pi^0 \gamma \gamma$  is dominated by the pion pole its branching ratio depends strongly on the value of the cut  $\delta m$ .

DAΦNE should be able to see both these decays, which have not been observed yet.

| $\delta m$ (MeV) | $BR(K_S \rightarrow \pi^0 \pi^0 \gamma \gamma)$ | $BR(K_L \rightarrow \pi^0 \pi^0 \gamma \gamma)$ |
|------------------|---|---|
| 5                | $5.6 \cdot 10^{-9}$                             | $2.0 \cdot 10^{-7}$                             |
| 10               | $5.3 \cdot 10^{-9}$                             | $8.4 \cdot 10^{-8}$                             |
| 20               | $4.7 \cdot 10^{-9}$                             | $3.0 \cdot 10^{-8}$                             |
| 30               | $4.0 \cdot 10^{-9}$                             | $1.4 \cdot 10^{-8}$                             |
| 40               | $3.4 \cdot 10^{-9}$                             | $6.4 \cdot 10^{-9}$                             |

Table 5:  $K_{L,S} \rightarrow \pi^0 \pi^0 \gamma \gamma$  branching ratios for different values of the cuts in the two-photon invariant mass ( $M_{\gamma\gamma} > \delta m$  and  $|M_{\gamma\gamma} - M_\pi| > \delta m$ ).

## 2.7 $K^+ \rightarrow \pi^+ \pi^0 \gamma \gamma$

We finally mention this decay which will probably not be observed at DAΦNE. Differently from the two-photon decays discussed above, a bremsstrahlung amplitude is present in this case. In agreement with the general statement of Eq. (1.8), this is the only contribution in CHPT at  $O(p^2)$ .

From the experimental point of view, it is again necessary to make a cut in the two-photon invariant mass in order to avoid the background from  $K^+ \rightarrow \pi^+ \pi^0 \pi^0$ . For  $M_{\gamma\gamma} > 170$  MeV the bremsstrahlung amplitude, which is suppressed by the  $\Delta I = 1/2$  rule, leads to a branching ratio of the order of  $10^{-10}$  [10].

At  $O(p^4)$  in CHPT, there is also a direct emission amplitude which, analogously to the  $K^+ \rightarrow \pi^+ \gamma \gamma$  case, has both anomalous and non-anomalous contributions. The latter depend on the scale independent combinations

$$N_{14} - N_{15} - N_{16} - N_{17} \quad \text{and} \quad N_{14} - N_{15} - 2N_{18} , \quad (2.41)$$

while the former depend on the combination  $a_3 - a_2/2$  [10] (see Sect. 1). Although it would be very useful to extract the counterterm combinations (2.41) from this decay, the direct emission and the interference amplitudes lead to branching ratios which are of  $O(10^{-10})$  [10]. DAΦNE will probably only put an upper limit on this decay.

## 2.8 CP violation

The charge asymmetry in the decays  $K^\pm \rightarrow \pi^\pm \gamma \gamma$  is an interesting observable for detecting direct CP violation. The amplitude for  $K^- \rightarrow \pi^- \gamma \gamma$  is obtained from (2.30) and (2.31) by replacing  $G_8$  and  $\hat{c}$  (defined in (2.32)) by their complex conjugates. The interference between the imaginary part of  $\hat{c}$  and the CP invariant absorptive part of the amplitude (2.30) generates a charge asymmetry [7]

$$\Delta\Gamma = \Gamma(K^+ \rightarrow \pi^+ \gamma \gamma) - \Gamma(K^- \rightarrow \pi^- \gamma \gamma)$$

$$\begin{aligned}
&= \frac{\text{Im}\hat{c}|G_8\alpha|^2 M_{K^+}^5}{2^{10}\pi^5} \int_{4r_\pi^2}^{(1-r_\pi)^2} dz \lambda^{\frac{1}{2}}(1, z, r_\pi^2)(r_\pi^2 - 1 - z) z \text{Im}F(z/r_\pi^2) \\
&\simeq 1.5 \cdot 10^{-20} \text{Im}\hat{c} \text{ MeV} .
\end{aligned} \tag{2.42}$$

For an estimate of  $\Delta\Gamma$  we need some information about the imaginary part of the counterterm combination  $\hat{c}$ . It is clear that  $L_9$  and  $L_{10}$  cannot contribute to this quantity. Furthermore, the long-distance contribution to the phase of the weak counterterm is already included in  $G_8$ . Therefore,  $\text{Im}\hat{c}$  is governed by the short-distance contribution to  $N_{14} - N_{15} - 2N_{18}$  [7], mainly due to the electromagnetic penguin operator [46]. The original estimate of Ref. [7] included only the contribution to  $\text{Im}N_{14}$  leading to the order-of-magnitude estimate

$$|\text{Im}\hat{c}| \sim 3 \cdot 10^{-3} . \tag{2.43}$$

However, it was later shown by Bruno and Prades [17] that there is also a contribution to  $\text{Im}N_{18}$  which in fact cancels  $\text{Im}N_{14}$  to leading order in  $1/N_c$ . Thus, the charge asymmetry is probably much smaller than the original estimate of Ref. [7] and certainly beyond reach for DAΦNE:

$$\frac{\Delta\Gamma(K^\pm \rightarrow \pi^\pm \gamma\gamma)}{2\Gamma(K^\pm \rightarrow \pi^\pm \gamma\gamma)} \ll 10^{-3} . \tag{2.44}$$

CP violation in  $K_L \rightarrow \gamma\gamma$  could also be interesting [1, 55]. As for  $K \rightarrow \pi\pi$ , one can separate direct and indirect CP violating contributions defining

$$\eta_{\parallel} = \frac{A(K_L \rightarrow 2\gamma_{\parallel})}{A(K_S \rightarrow 2\gamma_{\parallel})} \equiv \epsilon + \epsilon'_{\gamma\parallel} , \quad \eta_{\perp} = \frac{A(K_S \rightarrow 2\gamma_{\perp})}{A(K_L \rightarrow 2\gamma_{\perp})} \equiv \epsilon + \epsilon'_{\gamma\perp} . \tag{2.45}$$

While  $\epsilon'_{\gamma\parallel} \simeq \epsilon'_{\pi\pi}$ , the direct CP violating parameter  $\epsilon'_{\gamma\perp}$  could be substantially larger than  $\epsilon'_{\pi\pi}$  [29, 25, 50]. As shown in [56, 57], it is possible to study CP violation through time asymmetries in this channel, but statistics at DAΦNE does not seem to be large enough.

## 2.9 Improvements at DAΦNE

The measurements of the  $K_S \rightarrow \gamma\gamma$  and  $K_L \rightarrow \pi^0\gamma\gamma$  branching ratios will be sensitive to contributions of  $O(p^6)$  in CHPT. In particular, the study of the  $K_L \rightarrow \pi^0\gamma\gamma$  spectrum will be very useful to understand the role of resonances, the convergence of the CHPT expansion and to improve the predictions for the CP conserving contributions to  $K_L \rightarrow \pi^0 e^+ e^-$ .

In the decay  $K^+ \rightarrow \pi^+ \gamma\gamma$ , it will be important to determine the  $O(p^4)$  counterterm combination  $N_{14} - N_{15} - 2N_{18}$  and to check the correlation between the rate and the shape of the  $2\gamma$  spectrum.

Finally, the detection of the yet unobserved decays  $K_S \rightarrow \pi^0\gamma\gamma$  and  $K_{L,S} \rightarrow \pi^0\pi^0\gamma\gamma$  will furnish new important tests of CHPT, both in the anomalous and in the non-anomalous sectors.



### 3 Kaon decays with one photon in the final state

#### 3.1 Matrix elements and decay rates

The amplitude for  $K(P) \rightarrow \pi_1(p_1) + \pi_2(p_2) + \gamma(q)$  is decomposed into an electric amplitude  $E(x_i)$  and a magnetic amplitude  $M(x_i)$ :

$$A(K \rightarrow \pi_1 \pi_2 \gamma) = \varepsilon^\mu(q)^* [E(x_i)(p_1 q p_{2\mu} - p_2 q p_{1\mu}) + M(x_i)\varepsilon_{\mu\nu\rho\sigma} p_1^\nu p_2^\rho q^\sigma] / M_K^3, \quad (3.1)$$

$$x_i = \frac{P p_i}{M_K^2} \quad (i = 1, 2), \quad x_3 = \frac{P q}{M_K^2}, \quad x_1 + x_2 + x_3 = 1.$$

The invariant amplitudes  $E(x_i)$ ,  $M(x_i)$  are dimensionless. Summing over the photon helicity, the differential decay distribution can be written as ( $r_i = M_{\pi_i}/M_K$ )

$$\begin{aligned} \frac{d\Gamma}{dx_1 dx_2} &= \frac{M_K}{4(4\pi)^3} (|E(x_i)|^2 + |M(x_i)|^2) \times \\ &\times [(1 - 2x_3 - r_1^2 - r_2^2)(1 - 2x_1 + r_1^2 - r_2^2)(1 - 2x_2 + r_2^2 - r_1^2) \\ &- r_1^2(1 - 2x_1 + r_1^2 - r_2^2)^2 - r_2^2(1 - 2x_2 + r_2^2 - r_1^2)^2] . \end{aligned} \quad (3.2)$$

There is no interference between  $E$  and  $M$  as long as the photon helicity is not measured.

#### 3.2 Low's theorem and the chiral expansion

The behaviour of the electric amplitude in the limit of small photon energies ( $E_\gamma \rightarrow 0$ ) is governed by Low's theorem [58].  $E(x_i)$  can be written as the sum of a bremsstrahlung part  $E_B(x_i)$  and a direct emission part  $E_{DE}(x_i)$ ,

$$E(x_i) = E_B(x_i) + E_{DE}(x_i), \quad (3.3)$$

where the dependence on the photon energy is of the form

$$E_B(x_i) \sim 1/E_\gamma^2, \quad E_{DE}(x_i) = \text{const.} + O(E_\gamma). \quad (3.4)$$

The bremsstrahlung term  $E_B(x_i)$  is given by

$$\begin{aligned} E_B(x_i) &= \frac{e M_K^3 A(K \rightarrow \pi_1 \pi_2)}{P q} \left( \frac{Q_2}{p_2 q} - \frac{Q_1}{p_1 q} \right) \\ &= \frac{2e A(K \rightarrow \pi_1 \pi_2)}{M_K x_3} \left( \frac{Q_2}{1 + r_1^2 - r_2^2 - 2x_1} - \frac{Q_1}{1 + r_2^2 - r_1^2 - 2x_2} \right), \end{aligned} \quad (3.5)$$

where  $eQ_i$  is the electromagnetic charge of  $\pi_i$ .  $E_B(x_i)$  is thus completely determined by the amplitude for the decay  $K \rightarrow \pi_1 \pi_2$ .

This shows that to lowest  $O(p^2)$  in CHPT the  $K \rightarrow \pi_1\pi_2\gamma$  amplitudes are completely determined by  $E_B(x_i)$ . In other words, there is no additional information at  $O(p^2)$  that would not already be contained in the corresponding non-radiative transitions  $K \rightarrow \pi_1\pi_2$ . Contributions to  $E_{DE}(x_i)$  and  $M(x_i)$  can only show up at the next-to-leading  $O(p^4)$  in the chiral expansion. Of course, also  $E_B(x_i)$  receives corrections from  $A(K \rightarrow \pi_1\pi_2)|_{O(p^4)}$  at this chiral order.

### 3.3 $K_{L,S} \rightarrow \pi^0\pi^0\gamma$

For the decays  $K^0 \rightarrow \pi^0\pi^0\gamma$ , Bose statistics implies

$$\begin{aligned} E(x_2, x_1) &= -E(x_1, x_2) \\ M(x_2, x_1) &= -M(x_1, x_2) . \end{aligned} \quad (3.6)$$

In the limit where CP is conserved, the amplitude for  $K_L(K_S)$  is purely electric (magnetic).

The transition  $K_L \rightarrow \pi^0\pi^0\gamma$  has recently been considered in the literature [21, 59]. Eq. (3.6) implies the absence of a local amplitude of  $O(p^4)$ , or more generally the absence of an E1 amplitude. Although this by itself does not imply a vanishing one-loop amplitude (as can be seen in the case of  $K_L \rightarrow \pi^+\pi^-\gamma$  later in this section), Funck and Kambor [21] have shown that it does indeed vanish.

Thus, the decay  $K_L \rightarrow \pi^0\pi^0\gamma$  is at least  $O(p^6)$  in CHPT. In fact, chiral symmetry permits local octet couplings of  $O(p^6)$  contributing to this transition. A typical such term, considered in Ref. [10] with a coupling strength suggested by chiral dimensional analysis [60], gives rise to a branching ratio

$$BR(K_L \rightarrow \pi^0\pi^0\gamma)|_{O(p^6)} = 7 \cdot 10^{-11} . \quad (3.7)$$

By relating  $K_L \rightarrow \pi^0\pi^0\gamma$  to the decay  $K_L \rightarrow \pi^+\pi^-\gamma$  (which is dominantly M1), Heiliger and Sehgal obtain a considerably bigger estimate [59]  $BR(K_L \rightarrow \pi^0\pi^0\gamma)|_{\text{HS}} = 1 \cdot 10^{-8}$  together with  $BR(K_S \rightarrow \pi^0\pi^0\gamma)|_{\text{HS}} = 1.7 \cdot 10^{-11}$ .

### 3.4 $K_S \rightarrow \pi^+\pi^-\gamma$

In the limit of CP conservation, the amplitudes for  $K_S \rightarrow \pi^+\pi^-\gamma$  obey the symmetry relations

$$\begin{aligned} E(x_-, x_+) &= E(x_+, x_-) \\ M(x_-, x_+) &= -M(x_+, x_-) . \end{aligned} \quad (3.8)$$

To  $O(p^4)$ , the amplitude is therefore purely electric.

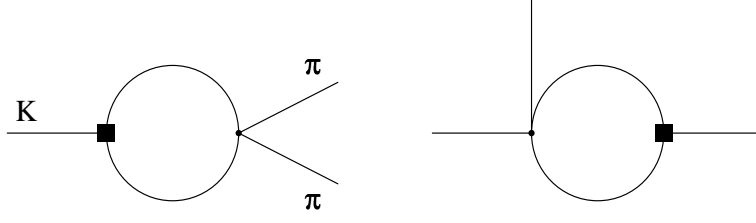


Figure 10: One-loop diagrams for  $K \rightarrow \pi\pi\gamma$ . The photon has to be attached to any charged line or to any vertex.

According to Sect. 3.2, the amplitude of  $O(p^2)$  is completely determined by bremsstrahlung:

$$E_B(x_i) = -\frac{eA(K_1^0 \rightarrow \pi^+\pi^-)}{M_K(\frac{1}{2} - x_+)(\frac{1}{2} - x_-)}, \quad p_1 = p_+, \quad p_2 = p_- . \quad (3.9)$$

At  $O(p^4)$ , the local contribution to the direct emission amplitude  $E_{DE}(x_i)$  is [61]

$$E_4^{\text{local}} = -\frac{4ieG_8M_K^3}{F}(N_{14} - N_{15} - N_{16} - N_{17}) . \quad (3.10)$$

The combination of coupling constants  $N_{14} - N_{15} - N_{16} - N_{17}$  is scale independent [12, 13] and it also appears in the electric amplitude for the decay  $K^+ \rightarrow \pi^+\pi^0\gamma$  [9, 10] (cf. Table 3). Consequently, the loop amplitudes for both  $K_S \rightarrow \pi^+\pi^-\gamma$  and  $K^+ \rightarrow \pi^+\pi^0\gamma$  are finite. The (dominant) pion loop amplitude for  $K_S \rightarrow \pi^+\pi^-\gamma$  (see Ref. [62] for the complete loop amplitude) is of the form [61, 62]:

$$E_4^{\text{pion loop}} = -\frac{ieG_8M_K^3}{\pi^2 F}(1 - r_\pi^2)H(z) , \quad z = 1 - 2x_3 , \quad (3.11)$$

where the function  $H(z)$  is defined in App. A.

At present, experimental data [2] are consistent with a pure bremsstrahlung amplitude. However, DAΦNE should be able to detect interference with the  $O(p^4)$  amplitude that is expected to show up at the level of  $10^{-5}$ – $10^{-6}$  in branching ratio (for  $E_\gamma > 20$  MeV) [61, 62].

### 3.5 $K_L \rightarrow \pi^+\pi^-\gamma$

The bremsstrahlung amplitude [9, 10] violates CP:

$$E_B(x_i) = -\frac{\varepsilon eA(K_1^0 \rightarrow \pi^+\pi^-)}{M_K(\frac{1}{2} - x_+)(\frac{1}{2} - x_-)}, \quad p_1 = p_+, \quad p_2 = p_- . \quad (3.12)$$

Here  $\varepsilon$  is the standard CP violation parameter in  $K \rightarrow \pi\pi$  decays and we have neglected  $\varepsilon'$ . This suppression of  $E_B(x_i)$  facilitates the experimental observation of the direct emission amplitude. From  $O(p^4)$  on we assume CP conservation implying

$$\begin{aligned} E(x_-, x_+) &= -E(x_+, x_-) \\ M(x_-, x_+) &= M(x_+, x_-) . \end{aligned} \quad (3.13)$$

The dominant contribution of  $O(p^4)$  occurs in the magnetic amplitude and it is due to the anomaly. As discussed in Sect. 1.3, there is no reducible anomalous amplitude of  $O(p^4)$ . The direct weak anomaly functional gives rise to [18, 10, 16]

$$M_4 = -\frac{eG_8 M_K^3}{2\pi^2 F}(a_2 + 2a_4) \quad (3.14)$$

in terms of the coupling constants  $a_i$  defined in (1.14).

Because of (3.13) there is no local contribution to the electric amplitude  $E(x_i)$  at  $O(p^4)$ . In contrast to  $K_L \rightarrow \pi^0 \pi^0 \gamma$ , there is however a finite one-loop amplitude which turns out [9, 10] to be very small,

$$\left| \frac{E_4^{\text{loop}}}{E_B} \right| \leq 1.2 \cdot 10^{-2} . \quad (3.15)$$

This small ratio is mainly due to the antisymmetry in  $x_+, x_-$  of  $E_4^{\text{loop}}$  dictated by CP invariance [cf. Eq. (3.13)].  $O(p^6)$  counterterms could substantially enhance the direct emission electric amplitude, which however could hardly be detected [62].

There are on the other hand strong experimental indications for the presence of a sizable magnetic amplitude beyond  $O(p^4)$ . A recent analysis of  $K_L \rightarrow \pi^+ \pi^- \gamma$  at FNAL [63] confirms an earlier result from Brookhaven [64] finding evidence for a dependence of the direct emission amplitude on the photon energy. On the other hand, the dominant direct emission amplitude  $M_4$  in (3.14) is a constant, independent of the photon energy.

At  $O(p^6)$ , CP invariance leads to the following most general form of the magnetic amplitude via Eq. (3.13):

$$M_6(x_+, x_-) = a + b(x_+ + x_-) = a + b - bx_3 = \widehat{M}_6 - bx_3 , \quad x_3 = \frac{Pq}{M_K^2} = \frac{E_\gamma}{M_K} . \quad (3.16)$$

To  $O(p^6)$ , the total magnetic amplitude is therefore given by

$$M(x_+, x_-) = M_4 + M_6(x_+, x_-) = M_4 + \widehat{M}_6 - bx_3 = (M_4 + \widehat{M}_6)(1 + cx_3) . \quad (3.17)$$

From the distribution in  $E_\gamma$  measured by E731 [63], one can extract [65] a value

$$c = -1.7 \pm 0.5 \quad (3.18)$$

for the slope  $c$ , in agreement with the earlier measurement [64, 66].

The dominant contributions of  $O(p^6)$  in CHPT were analysed in [10]. First of all, there is a reducible amplitude due to the anomaly of the form

$$M_6^{\text{anom}} = \frac{eG_8 M_K^3}{2\pi^2 F} F_1, \quad (3.19)$$

$$F_1 = \frac{1}{1 - r_\pi^2} - \frac{(c_\Theta - \sqrt{2}s_\Theta)(c_\Theta + 2\sqrt{2}\rho s_\Theta)}{3(r_\eta^2 - 1)} + \frac{(\sqrt{2}c_\Theta + s_\Theta)(2\sqrt{2}\rho c_\Theta - s_\Theta)}{3(r_{\eta'}^2 - 1)}$$

$$r_i = M_i/M_K, \quad c_\Theta = \cos \Theta, \quad s_\Theta = \sin \Theta.$$

In this formula,  $\Theta$  denotes the  $\eta$ - $\eta'$  mixing angle and  $\rho \neq 1$  takes into account possible deviations from nonet symmetry for the non-leptonic weak vertices (nonet symmetry is assumed for the strong WZW vertices). At  $O(p^4)$  ( $\Theta = 0$ ,  $M_{\eta'} \rightarrow \infty$ ),  $F_1$  vanishes because of the Gell-Mann–Okubo mass formula. In the real world, the  $\eta$  and  $\eta'$  contributions interfere destructively for  $0 \leq \rho < 1$  and  $\Theta \simeq -20^\circ$  as in the similar case of the  $K_L \rightarrow 2\gamma$  amplitude (cf. Sect. 2). Although not really predictable with any precision,  $F_1$  is dominated by the pion pole and certainly positive.

Vector meson exchange also enters at  $O(p^6)$ . There is a unique (for  $M_\pi = 0$ ) reducible amplitude originating from the strong VMD amplitude of  $O(p^6)$  via a weak rotation [9, 10]:

$$M_6^{\text{VMD}} = 2C_V(1 - 3x_3), \quad C_V = -\frac{16\sqrt{2}eG_8 g_V h_V M_K^5}{3M_V^2 F} \quad (M_V = M_\rho). \quad (3.20)$$

The vector meson couplings  $g_V$ ,  $h_V$  [15, 67] are approximately

$$g_V \simeq \frac{F_\pi}{\sqrt{2} M_V}, \quad |h_V| \simeq 3.7 \cdot 10^{-2}. \quad (3.21)$$

However, there is also a model-dependent direct weak amplitude of  $O(p^6)$  related to  $V$  exchange. In the factorization model [13]

$$M_6^{\text{FM}} = 4k_f C_V x_3 - \frac{eG_8 M_K^5 L_9}{\pi^2 F^3} k_f (2 - 5x_3), \quad (3.22)$$

where  $k_f$  is a fudge factor which naive factorization puts equal to one [ $k_f = 1$  corresponds to  $a_i = 1$  ( $i = 1, \dots, 4$ ) in Eq. (1.14)]. Altogether, one obtains [10] for the magnetic amplitude

$$M(x_3) = -\frac{eG_8 M_K^3}{2\pi^2 F} \left\{ a_2 + 2a_4 - F_1 + r_V[1 + x_3(2k_f - 3)] + \frac{2L_9 M_K^2}{F^2} k_f (2 - 5x_3) \right\} \quad (3.23)$$

$$r_V = \frac{64\sqrt{2}\pi^2 g_V h_V M_K^2}{3M_V^2} \simeq 0.4 \simeq \frac{2L_9^r(M_\rho) M_K^2}{F_\pi^2}.$$

The recent measurement [63] of the direct emission branching ratio

$$BR(E_\gamma > 20 \text{ MeV})_{\text{DE}} = (3.19 \pm 0.16) \cdot 10^{-5} \quad (3.24)$$

can be used to determine the quantity  $a_2 + 2a_4 - F_1$  for given values of  $k_f$ . Then, the slope parameter  $c$  defined in (3.17) can be extracted from Eq. (3.23) both in magnitude and sign. The values for  $c$  obtained by such an analysis [10] are in agreement with the experimental result (3.18).

A compilation and a critical discussion of previous literature on  $K_L \rightarrow \pi^+\pi^-\gamma$  can be found in Ref. [10].

### 3.6 $K^+ \rightarrow \pi^+\pi^0\gamma$

The decay  $K^+ \rightarrow \pi^+\pi^0\gamma$  shares several features with  $K_L \rightarrow \pi^+\pi^-\gamma$ :

- The bremsstrahlung amplitude is suppressed;
- The dominating contribution of  $O(p^4)$  is due to the chiral anomaly;
- The one-loop amplitude is finite, but again very small.

The bremsstrahlung amplitude [9, 10] is the complete amplitude of  $O(p^2)$  and it is suppressed by the  $\Delta I = 1/2$  rule:

$$E_B(x_i) = -\frac{eA(K^+ \rightarrow \pi^+\pi^0)}{M_K x_3(\frac{1}{2} - x_0)}, \quad p_1 = p_+, \quad p_2 = p_0. \quad (3.25)$$

The magnetic amplitude of  $O(p^4)$  consists of both a reducible and a direct amplitude [9, 18]:

$$M_4 = -\frac{eG_8 M_K^3}{2\pi^2 F} \left( -1 + \frac{3}{2}a_2 - 3a_3 \right). \quad (3.26)$$

Factorization suggests constructive interference between these two terms.

In contrast to  $K_L \rightarrow \pi^+\pi^-\gamma$ , there is now a local scale independent contribution of  $O(p^4)$  to the electric amplitude [9, 10]:

$$E_4^{\text{local}} = -\frac{2ieG_8 M_K^3}{F} (N_{14} - N_{15} - N_{16} - N_{17}). \quad (3.27)$$

As can be seen in Table 3, the same combination of coupling constants appears in the amplitude for  $K_S \rightarrow \pi^+\pi^-\gamma$  (Sect. 3.4). By measuring the energy spectrum of the photon, the counterterm amplitude (3.27) can in principle be isolated through its interference with the bremsstrahlung amplitude (3.25). One can estimate the size of this interference by appealing to the factorization model which predicts [13]

$$N_{14} - N_{15} - N_{16} - N_{17} = -k_f \frac{F_\pi^2}{2M_V^2} = -7 \cdot 10^{-3} k_f. \quad (3.28)$$

For  $k_f > 0$ , the interference is positive [9, 10]:

$$\frac{E_4^{\text{local}}}{E_B} \simeq 2.3x_3(1 - 2x_0)(-N_{14} + N_{15} + N_{16} + N_{17})/7 \cdot 10^{-3} . \quad (3.29)$$

The sign is well-determined because the ratio  $G_8/G_{27}$  is known to be positive from  $K \rightarrow 2\pi$  decays [see Eq. (1.6)]. Except for small  $E_\gamma$  ( $x_3 \rightarrow 0$ ,  $2x_0 \rightarrow 1$ ) where bremsstrahlung is bound to dominate, the amplitude  $E_4^{\text{local}}$  should be detectable. In fact, the experiment of Abrams et al. [68] is consistent with constructive interference between  $E_B$  and  $E_4^{\text{local}}$ , but the available data are not precise enough to separate the amplitudes  $E - E_B$  and  $M$  experimentally.

Since the counterterm amplitude (3.27) is scale independent, the loop amplitude must be finite. As in the case of  $K_L \rightarrow \pi^+\pi^-\gamma$ , its contribution is again very small [10, 62],

$$\left| \frac{E_4^{\text{loop}}}{E_B} \right| \leq 4.4 \cdot 10^{-2} . \quad (3.30)$$

At least in the foreseeable future, the loop amplitude can safely be neglected in comparison with the bremsstrahlung amplitude (3.25). On the other hand, the counterterm amplitude (3.27) should be within reach of experiments at DAΦNE.

For  $K_L \rightarrow \pi^+\pi^-\gamma$ , it was essential to include  $V$  exchange effects of  $O(p^6)$ , in particular to understand the slope parameter  $c$ . All the mechanisms discussed there also contribute to  $K^+ \rightarrow \pi^+\pi^0\gamma$ . Including the  $O(p^4)$  amplitude (3.26), the total magnetic amplitude is [10]

$$M = M_4 + M_6 \\ = -\frac{eG_8M_K^3}{4\pi^2F} \left\{ -2 + 3a_2 - 6a_3 + r_V(2k_f - 1) + \frac{2L_9M_K^2}{F^2}k_f(3 - 8x_+ - 2x_0) \right\} . \quad (3.31)$$

Under the assumption that direct emission is entirely due to the magnetic part, experiments [2, 68] find a branching ratio

$$BR(55 < T_{\pi^+}(\text{MeV}) < 90) = (1.8 \pm 0.4) \cdot 10^{-5} \quad (3.32)$$

for the given cuts in the kinetic energy of the charged pion. Proceeding in a similar way as for  $K_L \rightarrow \pi^+\pi^-\gamma$ , the quantity  $A_4 = -2 + 3a_2 - 6a_3$  can be extracted from the measured rate. For the values of  $r_V$  and  $L_9$  listed in Eq. (3.23),  $A_4$  is found to be [10]

$$A_4 = -4.1 - 0.3k_f \pm 0.5 , \quad 0 \leq k_f \leq 1 . \quad (3.33)$$

The following conclusions can be drawn:

- Compared with  $K_L \rightarrow \pi^+\pi^-\gamma$ , the  $V$  exchange contributions are of less importance in the present case. Especially for  $k_f \simeq 1$ , the  $O(p^6)$  terms are essentially negligible in the rate.

- The last term in Eq. (3.31) shows a rather pronounced dependence on  $x_+$ . A high-precision analysis of the decay distribution in  $T_{\pi^+}$  may be able to reveal this dependence.
- The fitted values of  $A_4$  are very much consistent with our expectations based on  $a_i \leq 1$  (cf. Sect. 1.3).
- Because of the expected positive interference between  $E_B$  and  $E_4^{\text{local}}$ , the coefficient  $|A_4|$  is probably somewhat smaller than found above. Future experimental analysis at DAΦNE should include an E1 amplitude of the type (3.27).

### 3.7 CP violation

The charge asymmetry in  $K^\pm \rightarrow \pi^\pm \pi^0 \gamma$  is a very promising observable for the detection of direct CP violation in radiative kaon decays. Although suppressed by the electromagnetic coupling, this channel may be competitive with  $K \rightarrow \pi\pi$  since it is not suppressed by the  $\Delta I = 1/2$  rule. CP violation in  $K^\pm \rightarrow \pi^\pm \pi^0 \gamma$  arises, like in the  $K^\pm \rightarrow \pi^\pm \gamma \gamma$  case, from the interference between the absorptive part of the electric amplitude (starting only at  $O(p^4)$ ) and the imaginary part of the counterterm contribution (3.27). As in the case of  $K^\pm \rightarrow \pi^\pm \gamma \gamma$ , the imaginary part of the weak counterterm is generated at short distances.

The authors of Ref. [69] claimed that the electric dipole operator could give a large contribution to the imaginary part of the weak counterterms, obtaining the following estimate:

$$\frac{\Delta\Gamma(K^\pm \rightarrow \pi^\pm \pi^0 \gamma)}{2\Gamma(K^\pm \rightarrow \pi^\pm \pi^0 \gamma)} \leq 1 \cdot 10^{-3} . \quad (3.34)$$

This estimate seems to be too optimistic since the counterterm introduced in Ref. [69] is of  $O(p^6)$  and does not have the correct chiral suppression factor. A more realistic estimate for the charge asymmetry is  $\Delta\Gamma/2\Gamma \sim 10^{-5}$  [70]. In any case, also with the large estimate of Eq. (3.34), DAΦNE will not have enough statistics to establish  $\Delta\Gamma \neq 0$  and will only put an interesting upper limit on the asymmetry.

A possible goal for DAΦNE could be to improve the measurement of

$$\eta_{+-\gamma} = \frac{A(K_L \rightarrow \pi^+ \pi^- \gamma)_{IB+E1}}{A(K_S \rightarrow \pi^+ \pi^- \gamma)_{IB+E1}} \quad (3.35)$$

which has already been observed at Fermilab [71]:

$$|\eta_{+-\gamma}| = \left| \frac{A(K_L \rightarrow \pi^+ \pi^- \gamma)_{IB+E1}}{A(K_S \rightarrow \pi^+ \pi^- \gamma)_{IB+E1}} \right| = (2.15 \pm 0.26 \pm 0.20) \times 10^{-3} , \quad (3.36)$$

$$\phi_{+-\gamma} = \arg \left\{ \frac{A(K_L \rightarrow \pi^+ \pi^- \gamma)_{IB+E1}}{A(K_S \rightarrow \pi^+ \pi^- \gamma)_{IB+E1}} \right\} = (72 \pm 23 \pm 17)^\circ . \quad (3.37)$$

DAΦNE should be able to improve these values studying the time evolution of the decay [72, 57].



### 3.8 Improvements at DAΦNE

The detection of both charged and neutral  $K \rightarrow \pi\pi\gamma$  decays with high statistics in the same experimental setup will lead to several interesting tests of CHPT.

The measurements of the electric direct emission components of  $K_S \rightarrow \pi^+\pi^-\gamma$  and  $K^+ \rightarrow \pi^+\pi^0\gamma$ , where the same counterterm combination appears, will furnish a consistency check of the  $O(p^4)$  contributions. Moreover, the measurements of the photon energy spectrum in  $K_L \rightarrow \pi^+\pi^-\gamma$  will lead to a substantial improvement in the determination of the slope parameter which is sensitive to contributions of  $O(p^6)$ . This will allow for checks of theoretical models.

## 4 Kaon decays with a lepton pair in the final state

We confine the discussion to final states with charged leptons only. Decays with a neutrino pair in the final state are of great theoretical interest and we refer to Ref. [1] for detailed reviews of both theoretical and experimental aspects. However, DAΦNE will not be able to gather significant statistics for  $K^+ \rightarrow \pi^+\nu\bar{\nu}$  with a branching ratio around  $10^{-10}$ , not to speak of the CP violating process  $K_L \rightarrow \pi^0\nu\bar{\nu}$ .

The decays with a Dalitz pair are in general dominated by one-photon exchange. This is certainly the case for transitions that occur already for a real photon like  $K^0 \rightarrow l^+l^-\gamma$ , but also for many decays that vanish for  $q^2 = 0$  like  $K \rightarrow \pi l^+l^-$  or  $K_L \rightarrow \pi^0\pi^0 l^+l^-$ . The decays  $K^0 \rightarrow l^+l^-$ , on the other hand, are dominated by two-photon exchange. For the consideration of CP violating effects, genuine short-distance mechanisms like  $Z$ -penguin and  $W$ -box diagrams must be taken into account. However, experiments at DAΦNE will only be able to give limits for CP violating observables for the class of decays considered in this section.

### 4.1 No pions in the final state

#### 4.1.1 $K^0 \rightarrow \gamma^*\gamma^*$

For a transition

$$M(p) \rightarrow \gamma^*(q_1) + \gamma^*(q_2), \quad p^2 = M^2,$$

gauge invariance implies the following general decomposition of the amplitude [7]:

$$\begin{aligned} M^{\mu\nu}(q_1, q_2) = & \left( g^{\mu\nu} - \frac{q_1^\mu q_1^\nu}{q_1^2} - \frac{q_2^\mu q_2^\nu}{q_2^2} + \frac{q_1 \cdot q_2}{q_1^2 q_2^2} q_1^\mu q_2^\nu \right) M^2 a(q_1^2, q_2^2) \\ & + \left[ q_2^\mu q_1^\nu - q_1 \cdot q_2 \left( \frac{q_1^\mu q_1^\nu}{q_1^2} + \frac{q_2^\mu q_2^\nu}{q_2^2} - \frac{q_1 \cdot q_2}{q_1^2 q_2^2} q_1^\mu q_2^\nu \right) \right] b(q_1^2, q_2^2) \\ & + \varepsilon^{\mu\nu\rho\sigma} q_{1\rho} q_{2\sigma} c(q_1^2, q_2^2). \end{aligned} \quad (4.1)$$

Due to Bose symmetry, the invariant amplitudes  $a, b, c$  are symmetric functions of  $q_1^2, q_2^2$ . With CP conserved,  $a$  and  $b$  contribute to  $K_1^0 \rightarrow \gamma^* \gamma^*$  while  $c$  contributes to  $K_2^0 \rightarrow \gamma^* \gamma^*$ .

When one of the photons is on-shell ( $q_1^2 = 0$ ),  $M^{\mu\nu}$  is described by two invariant amplitudes:

$$M^{\mu\nu}(q_1, q_2) = (q_2^\mu q_1^\nu - q_1 \cdot q_2 g^{\mu\nu})b(0, q_2^2) + \varepsilon^{\mu\nu\rho\sigma} q_{1\rho} q_{2\sigma} c(0, q_2^2) . \quad (4.2)$$

The decay widths are

$$\begin{aligned} \Gamma(K_S \rightarrow \gamma\gamma) &= \frac{M_K^3}{32\pi} |b(0, 0)|^2 \\ \Gamma(K_L \rightarrow \gamma\gamma) &= \frac{M_K^3}{64\pi} |c(0, 0)|^2 \end{aligned} \quad (4.3)$$

when both photons are on-shell.

In terms of these widths for the on-shell decays, the differential rates for  $K_{L,S} \rightarrow \gamma l^+ l^-$  can be written

$$\frac{d\Gamma(K_{L(S)} \rightarrow \gamma l^+ l^-)}{dz} = \Gamma(K_{L(S)} \rightarrow \gamma\gamma) |R_{L(S)}(z)|^2 \frac{2\alpha}{3\pi} \frac{(1-z)^3}{z} \left(1 + \frac{2r_l^2}{z}\right) \sqrt{1 - \frac{4r_l^2}{z}} , \quad (4.4)$$

where

$$z = \frac{q_2^2}{M_K^2} , \quad r_l = \frac{m_l}{M_K} \quad (4r_l^2 \leq z \leq 1)$$

and  $R(z)$  is a form factor normalized to  $R(0) = 1$ .

$$K_S \rightarrow \gamma l^+ l^-$$

The form factor  $R_S(z)$  was calculated to  $O(p^4)$  in CHPT [7]:

$$R_S(z) = H(z)/H(0) \quad (4.5)$$

where the loop function  $H(z)$  can be found in App. A. The corresponding decay rates for the Dalitz pair modes normalized to  $\Gamma(K_S \rightarrow \gamma\gamma)$  are compared in Table 6 with phase space and with a dispersion model [73]. Only for the muon channel the predictions of the Standard Model to  $O(p^4)$  could in principle be discriminated. The same qualification applies to the spectra given by Eq. (4.4). Therefore, DAΦNE will not distinguish between phase space and the CHPT prediction, but it should permit detection of the electronic mode.

$$K_L \rightarrow \gamma l^+ l^-$$

For the  $K_L$  decays we face the problem already encountered in Sect. 2 that it is difficult to obtain a reliable prediction for  $K_L \rightarrow \gamma\gamma$  in CHPT. The amplitude is formally of  $O(p^6)$

|                            | $l = e$              | $l = \mu$            |
|----------------------------|----------------------|----------------------|
| Standard Model to $O(p^4)$ | $1.60 \cdot 10^{-2}$ | $3.75 \cdot 10^{-4}$ |
| dispersion model [73]      | $1.59 \cdot 10^{-2}$ | $3.30 \cdot 10^{-4}$ |
| phase space                | $1.59 \cdot 10^{-2}$ | $4.09 \cdot 10^{-4}$ |

Table 6: Normalized rates  $\Gamma(K_S \rightarrow \gamma l^+ l^-)/\Gamma(K_S \rightarrow \gamma\gamma)$

in the chiral expansion although it is numerically more like a typical  $O(p^4)$  amplitude. Because the cancellation at  $O(p^4)$  involves two rather big amplitudes,  $A(K_L \rightarrow \gamma\gamma)$  is very sensitive to the chiral corrections which include in particular  $\eta - \eta'$  mixing. Since there is at this time no complete calculation of  $K_L \rightarrow \gamma\gamma$  in CHPT to  $O(p^6)$ , we will instead use the experimental value of  $|A(K_L \rightarrow \gamma\gamma)|$  whenever needed in this section.

The reducible amplitude is given by a VMD contribution to the transitions  $P^0 \rightarrow \gamma l^+ l^-$  ( $P^0 = \pi^0, \eta_8, \eta_1$ ) supplemented by an external weak transition  $P^0 \rightarrow K_L$  induced by  $\mathcal{L}_2^{\Delta S=1}$ . To first order in  $z$ , one obtains [74]

$$R_L^{VMD}(z) = 1 + c_V \frac{M_K^2}{M_V^2} z, \quad M_V = M_\rho \quad (4.6)$$

where the coefficient

$$c_V = \frac{32\sqrt{2}\pi^2 f_V h_V}{3} \quad (4.7)$$

contains the chiral vector meson couplings  $f_V, h_V$  [67, 15]. Its absolute value is  $|c_V| = 0.94$  in agreement with the analysis of Ref. [75] for  $P^0 \rightarrow \gamma\gamma^*$  and with experiment, which requires in addition  $c_V > 0$ . However, there is as usual also a direct weak contribution of  $O(p^6)$  to  $K_L \rightarrow \gamma\gamma^*$  which is model dependent. The total form factor to first order in  $z$  is [74]

$$R_L(z) = 1 + (c_V + c_D) \frac{M_K^2}{M_V^2} z \quad (4.8)$$

with a direct weak coefficient  $c_D$ . Choosing the relative sign between  $c_D$  and  $c_V$  appropriately, the weak deformation model [15] predicts

$$b = 0.7$$

for the slope  $b$  defined via

$$R_L(z) = 1 + bz + O(z^2), \quad (4.9)$$

in agreement with the experimental result [76]

$$b_{exp} = 0.67 \pm 0.11. \quad (4.10)$$

Thus, there is definitely experimental evidence for a direct weak amplitude interfering constructively with the VMD amplitude. A direct amplitude was already put forward in

Ref. [77] in terms of a  $\gamma^* - K^*$  transition. Their form factor has the form

$$R_L(z) = \frac{1}{1 - 0.418z} + \frac{c\alpha_{K^*}}{1 - 0.311z} \left[ \frac{4}{3} - \frac{1}{1 - 0.418z} - \frac{1}{9(1 - 0.405z)} - \frac{2}{9(1 - 0.238z)} \right] \quad (4.11)$$

where  $c$  was evaluated in terms of known coupling constants to be  $c = 2.5$  and  $\alpha_{K^*}$  parametrizes the unknown electroweak transition  $\gamma^* - K^*$ . In the vacuum insertion approximation the authors of Ref. [77] obtained  $|\alpha_{K^*}| \simeq 0.2 \sim 0.3$ . The experimental value (4.10) corresponds to  $\alpha_{K^*} = -0.28 \pm 0.12$ .

Once the slope is given, one can use (4.9) in (4.4) to predict the rate. The agreement with the experimental results

$$BR(K_L \rightarrow e^+e^-\gamma)_{\text{exp}} = \begin{cases} (9.2 \pm 0.5 \pm 0.5) \cdot 10^{-6} & [76] \\ (9.1 \pm 0.4 \pm_{-0.5}^{+0.6}) \cdot 10^{-6} & [78] \end{cases} \quad (4.12)$$

confirms that the linear approximation for  $R_L(z)$  is sufficient. DAΦNE will have more statistics for  $K_L \rightarrow \gamma e^+e^-$  and will also be able to measure  $K_L \rightarrow \gamma \mu^+\mu^-$ , where the dependence on the form factor is stronger. Both with a linear form factor (4.9) and with the VMD form factor (4.11) one arrives at essentially the same prediction [74, 77]

$$\frac{\Gamma(K_L \rightarrow \gamma e^+e^-)}{\Gamma(K_L \rightarrow \gamma \mu^+\mu^-)} \simeq 25. \quad (4.13)$$

$$K_L \rightarrow e^+e^-e^+e^-$$

The decay  $K_L \rightarrow e^+e^-e^+e^-$  is sensitive to the invariant amplitude  $c(q_1^2, q_2^2)$  in Eq. (4.1). There is no explicit theoretical calculation yet. DAΦNE will improve the existing value for the branching ratio

$$BR(K_L \rightarrow e^+e^-e^+e^-)_{\text{exp}} = (3.9 \pm 0.7) \cdot 10^{-8} [2] \quad (4.14)$$

and will test the  $K_L \rightarrow \gamma^*\gamma^*$  amplitude.

On the basis of Table 6, DAΦNE will not be able to see the corresponding decay  $K_S \rightarrow e^+e^-e^+e^-$ .

#### 4.1.2 $K^0 \rightarrow l^+l^-$

The amplitude for the decay of a  $K^0$  into a lepton pair has the general form

$$A(K^0 \rightarrow l^+l^-) = \bar{u}(iB + A\gamma_5)v \quad (4.15)$$

with a decay rate

$$\Gamma(K^0 \rightarrow l^+l^-) = \frac{M_K \beta_l}{8\pi} (|A|^2 + \beta_l^2 |B|^2), \quad \beta_l = \left(1 - \frac{4m_l^2}{M_K^2}\right)^{1/2}. \quad (4.16)$$

In the CP limit, the transition  $K_1^0 \rightarrow l^+l^-$  is determined by the  $p$ -wave amplitude  $B_1$  while  $K_2^0 \rightarrow l^+l^-$  proceeds only via the  $s$ -wave  $A_2$ .

There is a unique lowest-order coupling [79]

$$\partial^\mu K_2^0 \bar{\psi} \gamma_\mu \gamma_5 \psi \quad (4.17)$$

that contributes only to the  $s$ -wave amplitude  $A_2$ . There is in fact a well-known short-distance amplitude of this type for  $K_L \rightarrow l^+l^-$  [1] with an important top-quark contribution. However, this decay is dominated by the absorptive part of the transition  $K_L \rightarrow \gamma^* \gamma^* \rightarrow l^+l^-$ :

$$|\text{Im } A_2^{\gamma\gamma}| = \frac{\alpha m_\mu}{4\beta_\mu M_K} \ln \frac{1 + \beta_\mu}{1 - \beta_\mu} \left[ \frac{64\pi \Gamma(K_L \rightarrow 2\gamma)}{M_K} \right]^{1/2} \quad (4.18)$$

or

$$BR(K_L \rightarrow \mu^+ \mu^-)_{\text{abs}} \simeq \frac{\alpha^2 m_\mu^2}{2\beta_\mu M_K^2} \left( \ln \frac{1 + \beta_\mu}{1 - \beta_\mu} \right)^2 B(K_L \rightarrow 2\gamma). \quad (4.19)$$

The experimental branching ratio [2]  $BR(K_L \rightarrow 2\gamma) = (5.73 \pm 0.27) \cdot 10^{-4}$  yields

$$|\text{Im } A_2^{\gamma\gamma}| = (2.21 \pm 0.05) \cdot 10^{-12} \quad (4.20)$$

and

$$BR(K_L \rightarrow \mu^+ \mu^-)_{\text{abs}} = (6.85 \pm 0.32) \cdot 10^{-9}. \quad (4.21)$$

Comparing with the latest measurements

$$BR(K_L \rightarrow \mu^+ \mu^-) = \begin{cases} (7.9 \pm 0.6 \pm 0.3) \cdot 10^{-9} & \text{KEK-137 [80]} \\ (7.0 \pm 0.5) \cdot 10^{-9} & \text{BNL-E791 [81]} \\ (7.4 \pm 0.4) \cdot 10^{-9} & \text{PDG [2]} \end{cases}, \quad (4.22)$$

one finds that the absorptive part (unitarity bound) nearly saturates the total rate.

The dispersive part for the two-photon intermediate state is model dependent. There are various models in the literature [77, 82] that make different predictions for the dispersive part. As long as not even the sign of the interference between the dispersive and the short-distance part is established, the decay  $K_L \rightarrow \mu^+ \mu^-$  is of limited use for the determination of the CKM mixing matrix element  $V_{td}$ . Because of the helicity suppression, DAΦNE will not be able to see the decay  $K_L \rightarrow e^+ e^-$  [the unitarity bound due to the absorptive part is  $BR(K_L \rightarrow e^+ e^-) = 3 \cdot 10^{-12}$ ], unless there are contributions from mechanisms beyond the Standard Model.

The same statement applies to the decays  $K_S \rightarrow l^+ l^-$ . These decays are theoretically interesting because the lowest-order amplitude in CHPT is unambiguously calculable [79]. It is given by a two-loop diagram describing the transition  $K_1^0 \rightarrow \gamma^* \gamma^* \rightarrow l^+ l^-$ . The subprocess  $K_1^0 \rightarrow \gamma^* \gamma^*$  is determined by the one-loop diagrams in Fig. 1 relevant for  $K_S \rightarrow \gamma\gamma$  as discussed in Sect. 2.

Normalizing to the rate for  $K_S \rightarrow \gamma\gamma$ , one obtains the relative branching ratios [79]

$$\frac{\Gamma(K_S \rightarrow \mu^+ \mu^-)}{\Gamma(K_S \rightarrow \gamma\gamma)} = 2 \cdot 10^{-6} , \quad \frac{\Gamma(K_S \rightarrow e^+ e^-)}{\Gamma(K_S \rightarrow \gamma\gamma)} = 8 \cdot 10^{-9} , \quad (4.23)$$

well below the present experimental upper limits [2] and beyond the reach of DAΦNE.

## 4.2 $K \rightarrow \pi l^+ l^-$

$K \rightarrow \pi\gamma$  with a real photon is forbidden by gauge and Lorentz invariance. The CP conserving Dalitz pair decays  $K^+ \rightarrow \pi^+ l^+ l^-$  and  $K_1^0 \rightarrow \pi^0 l^+ l^-$  are dominated by virtual photon exchange. In accordance with the general theorem (1.7), the leading amplitudes for these transitions are of  $O(p^4)$  in CHPT. At this order, there are both one-loop contributions and tree level contributions involving the low-energy constants  $N_{14}$  and  $N_{15}$  [83]. The determination of these coupling constants will be one of the goals of experiments at DAΦNE.

The amplitude for

$$K(p) \rightarrow \pi(p') + \gamma^*(q) \rightarrow \pi(p') l^+(k') l^-(k) , \quad q = k + k' \quad (4.24)$$

has the general form compatible with Lorentz and gauge invariance

$$A(K \rightarrow \pi \gamma^* \rightarrow \pi l^+ l^-) = -\frac{G_8 e^2}{(4\pi)^2 (q^2 + i\epsilon)} V_\mu(p, q) \bar{u}(k) \gamma^\mu v(k') , \quad (4.25)$$

where

$$V_\mu(p, q) = [q^2(p + p')_\mu - (M_K^2 - M_\pi^2)q_\mu] V(z) , \quad z = \frac{q^2}{M_K^2} . \quad (4.26)$$

Within the one-photon exchange approximation, all the dynamics is contained in the invariant functions  $V_+(z)$  and  $V_S(z)$  for the decays  $K^+ \rightarrow \pi^+ l^+ l^-$  and  $K_S \rightarrow \pi^0 l^+ l^-$ , respectively. The differential decay rate is given by

$$\frac{d\Gamma}{dz} = \frac{G_8^2 \alpha^2 M_K^5}{192 \pi^5} \lambda^{3/2}(1, z, r_\pi^2) \left(1 - \frac{4r_l^2}{z^2}\right)^{1/2} \left(1 + \frac{2r_l^2}{z}\right) |V(z)|^2 \quad (4.27)$$

$$r_\pi = \frac{M_\pi}{M_K} , \quad r_l = \frac{m_l}{M_K} , \quad 4r_l^2 \leq z \leq (1 - r_\pi)^2 .$$

The kinematical function  $\lambda(x, y, z)$  is defined in App. A.

At  $O(p^4)$  in CHPT, the invariant amplitudes are [83]

$$\begin{aligned} V_+(z) &= -\varphi(z) - \varphi(z/r_\pi^2) - w_+ \\ V_S(z) &= 2\varphi(z) + w_S. \end{aligned} \quad (4.28)$$

The loop function  $\varphi(z)$  can be found in App. A. The scale independent constants  $w_+$  and  $w_S$  contain both strong and weak low-energy constants:

$$\begin{aligned} w_+ &= \frac{4}{3}(4\pi)^2 (N_{14}^r(\mu) - N_{15}^r(\mu) + 3L_9^r(\mu)) - \frac{1}{3} \ln \frac{M_K M_\pi}{\mu^2} \\ w_S &= \frac{2}{3}(4\pi)^2 (2N_{14}^r(\mu) + N_{15}^r(\mu)) - \frac{1}{3} \ln \frac{M_K^2}{\mu^2}. \end{aligned} \quad (4.29)$$

Note that the coupling constant  $N_{14}$  contains [83, 17] the electromagnetic penguin contribution [46]. The branching ratios are quadratic functions of these constants [83, 66]:

$$\begin{aligned} BR(K^+ \rightarrow \pi^+ e^+ e^-) &= (3.15 - 21.1w_+ + 36.1w_+^2) \cdot 10^{-8} |G_8/9 \cdot 10^{-6} \text{GeV}^{-2}|^2 \\ BR(K^+ \rightarrow \pi^+ \mu^+ \mu^-) &= (3.93 - 32.7w_+ + 70.5w_+^2) \cdot 10^{-9} |G_8/9 \cdot 10^{-6} \text{GeV}^{-2}|^2 \\ BR(K_S \rightarrow \pi^0 e^+ e^-) &= (3.07 - 18.7w_S + 28.4w_S^2) \cdot 10^{-10} |G_8/9 \cdot 10^{-6} \text{GeV}^{-2}|^2 \\ BR(K_S \rightarrow \pi^0 \mu^+ \mu^-) &= (6.29 - 38.9w_S + 60.1w_S^2) \cdot 10^{-11} |G_8/9 \cdot 10^{-6} \text{GeV}^{-2}|^2. \end{aligned} \quad (4.30)$$

So far, only the decay  $K^+ \rightarrow \pi^+ e^+ e^-$  has been observed. A recent experiment at Brookhaven [84] has reported both a branching ratio

$$BR(K^+ \rightarrow \pi^+ e^+ e^-) = (2.99 \pm 0.22) \cdot 10^{-7} \quad (4.31)$$

and a value

$$w_+ = 0.89_{-0.14}^{+0.24} \quad (4.32)$$

for the constant  $w_+$  from a fit to the spectrum shape. In principle, the branching ratio  $BR(K^+ \rightarrow \pi^+ e^+ e^-)$  depends very sensitively on  $w_+$ . However, due to the considerable uncertainty in the octet coupling  $G_8$ , the shape of the  $z$  distribution is at present a safer observable to extract  $w_+$ . Nevertheless, for the central value of  $G_8$  in Eq. (1.6) the value for  $w_+$  extracted from the rate agrees with (4.32) within  $1.5\sigma$  [84].

It was pointed out in Ref. [85] that the observation of a parity violating asymmetry in these decays would reveal the presence of a short-distance contribution ( $Z$ -penguin and  $W$ -box diagrams) interfering with the dominant one-photon exchange amplitude (4.25). The asymmetry could yield information on the CKM matrix element  $V_{td}$ . From the analysis of Ref. [85] one concludes that DAΦNE will only be able to place an upper limit on this asymmetry.

Since  $w_+$  and  $w_S$  depend on two different combinations of the weak low-energy constants  $N_{14}$  and  $N_{15}$ , chiral symmetry does not yield any relation between them. Consequently, chiral symmetry alone does not relate the decay amplitudes for  $K^+ \rightarrow \pi^+ l^+ l^-$

and  $K_S \rightarrow \pi^0 l^+ l^-$ . Starting with Ref. [83], several model assumptions have been proposed that would allow to express  $w_S$  in terms of  $w_+$  [15, 16, 13, 17]. As an example, we consider the factorization model [13] that predicts such a relation in terms of the parameter  $k_f$  encountered previously ( $0 < k_f \lesssim 1$ ):

$$w_S = w_+ + \frac{2(4\pi F_\pi)^2}{M_V^2}(2k_f - 1) + \frac{1}{3} \ln \frac{M_\pi}{M_K} = w_+ + 4.6(2k_f - 1) - 0.43 . \quad (4.33)$$

The original model of Ref. [83] had  $k_f = 1/2$  as also predicted by the weak deformation model [15]. As Eq. (4.33) indicates,  $w_S$  is extremely sensitive to small deviations from  $k_f = 1/2$  even within the specific factorization model. Moreover, for the experimental value (4.32) of  $w_+$  the relation (4.33) gives  $w_S \simeq 0.5$  for  $k_f = 1/2$ . In the invariant amplitude  $V_S(z)$  in (4.28), the function  $\varphi(z)$  due to the kaon loop varies very little over the physical region and is approximately given by  $\varphi(0) = -1/6$ . Thus, there is a strong destructive interference between the loop contribution and  $w_S$  in this case and the resulting branching ratio [83]  $BR(K_S \rightarrow \pi^0 e^+ e^-) \simeq 5 \cdot 10^{-10}$  is very small. Both in view of the strong model dependence and of possible higher-order chiral corrections, such a low rate should be interpreted as an approximate lower limit rather than as a reliable prediction. To emphasize this point, we also give the predictions of Ref. [17] for the two constants  $w_+$ ,  $w_S$ :

$$\begin{aligned} w_+ &= 1.0_{-0.4}^{+0.8} \\ w_S &= 1.0_{-0.6}^{+1.0} . \end{aligned} \quad (4.34)$$

It is evident that theory cannot make a reliable prediction for  $w_S$  at this time. On the other hand, DAΦNE should be able either to detect the decay  $K_S \rightarrow \pi^0 e^+ e^-$  or to give at least a non-trivial upper bound for  $|w_S|$ .

### 4.3 $K_L \rightarrow \pi^0 \pi^0 e^+ e^-$

If there is a non-vanishing  $O(p^4)$  amplitude for a process with a real photon, the corresponding Dalitz pair transition is usually dominated by the same mechanism. A typical example is the decay  $K_L \rightarrow \pi^+ \pi^- e^+ e^-$  [86, 87]. As discussed in Sect. 3, the amplitude for  $K_L \rightarrow \pi^+ \pi^- \gamma$  is mainly given by bremsstrahlung and by the magnetic amplitude  $M_4$  due to the chiral anomaly. It has been argued in Refs. [86, 87] that the additional loop contributions, which vanish for a real photon, are negligible for the Dalitz pair decay amplitude. The final result for the branching ratio is [87]

$$BR(K_L \rightarrow \pi^+ \pi^- e^+ e^-) = 2.8 \cdot 10^{-7} . \quad (4.35)$$

The situation is different for a transition like  $K_L \rightarrow \pi^0 \pi^0 l^+ l^-$  where the amplitude vanishes to  $O(p^4)$  for a real photon, but where a non-zero amplitude exists for virtual photons: there is a non-vanishing electric amplitude of  $O(p^4)$  to which both counterterms and loop diagrams contribute [21].



As can be seen from Table 3, the loop amplitude is divergent and the same combination of counterterms appears as in the decay  $K_S \rightarrow \pi^0 l^+ l^-$  discussed previously. The amplitude has the form

$$A(K_L \rightarrow \pi^0 \pi^0 l^+ l^-) = \Phi(q^2, p \cdot q) [p \cdot q q^\mu - q^2 p^\mu] \frac{e}{q^2} \bar{u}(q_1) \gamma_\mu v(q_2) \quad (4.36)$$

where  $p = p_1 + p_2$  is the sum of the pion momenta and  $q = q_1 + q_2$  is the virtual photon momentum. The invariant amplitude  $\Phi(q^2, p \cdot q)$  was calculated by Funck and Kambor [21]:

$$\begin{aligned} \Phi(q^2, p \cdot q) = & \frac{G_8 e}{16\pi^2 F} \left\{ \frac{2(M_K^2 - M_\pi^2)}{2p \cdot q + q^2} [\varphi(z) - \varphi\left(\frac{z}{r_\pi^2}\right) + \frac{1}{3} \ln r_\pi] \right. \\ & \left. + 2\varphi\left(\frac{z}{r_\pi^2}\right) - \frac{2}{3} \ln r_\pi + w_S \right\} \end{aligned} \quad (4.37)$$

$$r_\pi = \frac{M_\pi}{M_K}, \quad z = \frac{q^2}{M_K^2}$$

$$w_S = \frac{32\pi^2}{3} [2N_{14}^r(\mu) + N_{15}^r(\mu)] - \frac{1}{3} \ln \frac{M_K^2}{\mu^2}.$$

The function  $\varphi(z)$  can be found in App. A.

The authors of Ref. [21] have made a careful study of the total rate and of various spectra for different values of  $w_S$ . The situation is similar to  $K_S \rightarrow \pi^0 e^+ e^-$  discussed in Sect. 4.2. The rate is again very sensitive to the coupling constant  $w_S$ . The counterterm amplitude interferes constructively (destructively) with the loop amplitude for negative (positive)  $w_S$ . However, even with constructive interference the branching ratio is at most  $10^{-9}$ . DAΦNE will probably only set an upper limit for the rate.

## 4.4 CP violation

The possibility to study CP violation in  $K_L \rightarrow \pi^+ \pi^- e^+ e^-$  has been investigated recently [86, 87]. The employed model contains (i) a CP conserving amplitude associated with the M1 transition in  $K_L \rightarrow \pi^+ \pi^- \gamma$ , (ii) an indirect CP violating amplitude related to the bremsstrahlung part of  $K_L \rightarrow \pi^+ \pi^- \gamma$ , and (iii) a direct CP violating term associated with the short-distance interaction  $s\bar{d} \rightarrow e^+ e^-$ . Interference among the first two components generates a large CP violating asymmetry ( $\sim 14\%$ ) in the angle  $\phi$  between the planes of  $e^+ e^-$  and  $\pi^+ \pi^-$ . With the branching ratio (4.35), DAΦNE will measure the indirect CP violating contribution in this channel. The effects of direct CP violation are much smaller and not accessible for DAΦNE.

Other CP violating observables involving lepton pairs, like the decays  $K_L \rightarrow \pi^0 e^+ e^-$  and  $K_L \rightarrow \pi^0 \nu \bar{\nu}$  [88], the charge asymmetry in  $K^\pm \rightarrow \pi^\pm e^+ e^-$  and the transverse muon polarization in  $K_L \rightarrow \pi^0 \mu^+ \mu^-$  [7] are beyond the reach of DAΦNE.

## 4.5 Improvements at DAΦNE

DAΦNE should be able to improve the experimental information about the form factors in the decay  $K_L \rightarrow e^+e^-\gamma$ . Those measurements will serve as a test of different model predictions. One should also obtain a first measurement of  $K_L \rightarrow \mu^+\mu^-\gamma$ . However, due to the smaller number of events, it will be more difficult to discriminate between different models in this case.

On the other hand, statistics at DAΦNE should be sufficient to improve the measurement of the width and of the lepton spectrum in  $K^+ \rightarrow \pi^+e^+e^-$  and to detect the decay  $K^+ \rightarrow \pi^+\mu^+\mu^-$ .

A very interesting channel is  $K_S \rightarrow \pi^0e^+e^-$ , which is extremely sensitive to the counterterm amplitude. DAΦNE should be able to detect this decay and to discriminate among models for the counterterm coupling constants. This information will be especially important for the indirect CP violating contribution to  $K_L \rightarrow \pi^0e^+e^-$  [89].

## Acknowledgements

We want to thank our collaborators and the members of the DAΦNE working groups for their contributions and for their helpful comments, especially F. Buccella, L. Cappiello, A.G. Cohen, D. Espriu, J. Kambor, L. Maiani, M. Miragliuolo, N. Paver, A. Pich, A. Pugliese, E. de Rafael and F. Sannino. G.D. thanks the CERN Theory Division, where part of this work was done, for hospitality.

## A Loop functions

The following functions occur in one-loop amplitudes for the  $K$  decays discussed in this chapter:

$$F(z) = \begin{cases} 1 - \frac{4}{z} \arcsin^2(\sqrt{z}/2) & z \leq 4 \\ 1 + \frac{1}{z} \left( \ln \frac{1 - \sqrt{1 - 4/z}}{1 + \sqrt{1 - 4/z}} + i\pi \right)^2 & z \geq 4 \end{cases} \quad (\text{A.1})$$

$$G(z) = \begin{cases} \sqrt{4/z - 1} \arcsin(\sqrt{z}/2) & z \leq 4 \\ -\frac{1}{2} \sqrt{1 - 4/z} \left( \ln \frac{1 - \sqrt{1 - 4/z}}{1 + \sqrt{1 - 4/z}} + i\pi \right) & z \geq 4 \end{cases} \quad (\text{A.2})$$

$$\varphi(z) = \frac{5}{18} - \frac{4}{3z} - \frac{1}{3} \left(1 - \frac{4}{z}\right) G(z) \quad (\text{A.3})$$

$$H(z) = \frac{1}{2(1-z)^2} \left\{ z F\left(\frac{z}{r_\pi^2}\right) - F\left(\frac{1}{r_\pi^2}\right) - 2z \left[ G\left(\frac{z}{r_\pi^2}\right) - G\left(\frac{1}{r_\pi^2}\right) \right] \right\} \quad (\text{A.4})$$

$r_\pi = M_\pi/M_K$  .

The kinematical function  $\lambda(x, y, z)$  is defined as

$$\lambda(x, y, z) = x^2 + y^2 + z^2 - 2(xy + yz + zx) . \quad (\text{A.5})$$

## References

- [1] J.L. Ritchie and S.G. Wojcicki, *Rev. Mod. Phys.* 65 (1993) 1149;  
L. Littenberg and G. Valencia, *Ann. Rev. Nucl. Part. Sci.* 43 (1993) 729;  
A.J. Buras and M.K. Harlander, in “Heavy Flavours”, Eds. A.J. Buras and M. Lindner, *Advanced Series on Directions in High Energy Physics* (World Scientific, Singapore 1992), Vol. 10, p. 58;  
R. Battiston, D. Cocolicchio, G.L. Fogli and N. Paver, *Phys. Rep.* 214 (1992) 293;  
B. Winstein and L. Wolfenstein, *Rev. Mod. Phys.* 65 (1993) 1113.
- [2] Review of Particle Properties, *Phys. Rev. D* 50 (1994) vol. 3, part II.
- [3] P. Franzini, private communication.
- [4] J. Bijnens, G. Ecker and J. Gasser, “Introduction to chiral perturbation theory”, in this report and references therein.
- [5] M.K. Gaillard and B.W. Lee, *Phys. Rev. Lett.* 33 (1974) 108;  
G. Altarelli and L. Maiani, *Phys. Lett.* 52B (1974) 351;  
A.I. Vainshtein, V.I. Zakharov and M.A. Shifman, *JETP Lett.* 22 (1975) 55;  
M.A. Shifman, A.I. Vainshtein and V.I. Zakharov, *Nucl. Phys.* B120 (1977) 316;  
F.J. Gilman and M.B. Wise, *Phys. Rev. D* 20 (1979) 2392.
- [6] G. Ecker, A. Pich and E. de Rafael, *Phys. Lett.* B189 (1987) 363.
- [7] G. Ecker, A. Pich and E. de Rafael, *Nucl. Phys.* B303 (1988) 665.
- [8] E. de Rafael, *Nucl. Phys. B (Proc. Suppl.)* 7A (1989) 1.
- [9] G. Ecker, H. Neufeld and A. Pich, *Phys. Lett.* B278 (1992) 337.
- [10] G. Ecker, H. Neufeld and A. Pich, *Nucl. Phys.* B413 (1994) 321.
- [11] G. D’Ambrosio, G. Ecker and H. Neufeld, in preparation.
- [12] J. Kambor, J. Missimer and D. Wyler, *Nucl. Phys.* B346 (1990) 17.
- [13] G. Ecker, J. Kambor and D. Wyler, *Nucl. Phys.* B394 (1993) 101.
- [14] G. Ecker, “Geometrical aspects of the non-leptonic weak interactions of mesons”, in *Proc. of the IX. Int. Conference on the Problems of Quantum Field Theory, Dubna, April 1990*, Ed. M.K. Volkov (Dubna, 1990);  
G. Esposito-Farèse, *Z. Phys.* C50 (1991) 255.
- [15] G. Ecker, A. Pich and E. de Rafael, *Phys. Lett.* B237 (1990) 481.
- [16] H.-Y. Cheng, *Phys. Rev. D* 42 (1990) 72; *Phys. Lett.* B238 (1990) 399; *Phys. Rev. D* 43 (1991) 1579.

- [17] C. Bruno and J. Prades, Z. Phys. C57 (1993) 585.
- [18] J. Bijnens, G. Ecker and A. Pich, Phys. Lett. B286 (1992) 341.
- [19] J. Wess and B. Zumino, Phys. Lett. 37B (1971) 95;  
E. Witten, Nucl. Phys. B223 (1983) 422.
- [20] H. Dykstra, J.M. Flynn and L. Randall, Phys. Lett. B270 (1991) 45.
- [21] R. Funck and J. Kambor, Nucl. Phys. B396 (1993) 53.
- [22] A. Pich and E. de Rafael, Nucl. Phys. B358 (1991) 311.
- [23] S.L. Adler and W.A. Bardeen, Phys. Rev. 182 (1969) 1517.
- [24] G. D'Ambrosio and D. Espriu, Phys. Lett. B175 (1986) 237;  
J.I. Goity, Z. Phys. C34 (1987) 341.
- [25] F. Buccella, G. D'Ambrosio and M. Miragliuolo, Nuovo Cimento 104A (1991) 777.
- [26] H. Burkhardt et al. (CERN-NA31), Phys. Lett. B199 (1987) 139.
- [27] J. Kambor and B.R. Holstein, Phys. Rev. D49 (1994) 2346.
- [28] T.N. Truong, Phys. Lett. B313 (1994) 221.
- [29] L. L. Chau and H.-Y. Cheng, Phys. Rev. Lett. 54 (1985) 1768; Phys. Lett. B195 (1987) 275.
- [30] Z.E.S. Uy, Phys. Rev. D29 (1984) 574; Phys. Rev. D37 (1988) 2684; Phys. Rev. D43 (1991) 802; Phys. Rev. D43 (1991) 1572.
- [31] L. Cappiello and G. D'Ambrosio, Nuovo Cimento 99A (1988) 155.
- [32] L. Cappiello, G. D'Ambrosio and M. Miragliuolo, Phys. Lett. B298 (1993) 423.
- [33] P. Ko, Phys. Rev. D41 (1990) 1531.
- [34] T. Morozumi and H. Iwasaki, Progr. Theor. Phys. 82 (1989) 371.
- [35] L.M. Sehgal, Phys. Rev. D38 (1988) 808; Phys. Rev. D41 (1990) 1611.
- [36] P. Heiliger and L.M. Sehgal, Phys. Rev. D46 (1992) 1035.
- [37] M. K. Volkov, Czech. J. Phys. 41 (1991) 1053;  
S. Fajfer, Phys. Rev. D51 (1995) 1101.
- [38] J. F. Donoghue, B. R. Holstein and G. Valencia, Phys. Rev. D35 (1987) 2769.

- [39] C.O. Dib, I. Dunietz and F. J. Gilman, Phys. Lett. B218 (1989) 487; Phys. Rev. D39 (1989) 2639.
- [40] J. Flynn and L. Randall, Nucl. Phys. B326 (1989) 31.
- [41] G. Buchalla, A.J. Buras and M. Harlander, Nucl. Phys. B349 (1991) 1;  
A.J. Buras, M.E. Lautenbacher, M. Misiak and M. Münz, Nucl. Phys. B423 (1994) 349.
- [42] G.D. Barr et al. (CERN-NA31), Phys. Lett. B284 (1992) 440.
- [43] V. Papadimitriou et al. (FNAL-E731), Phys. Rev. D44 (1991) 573.
- [44] J.F. Donoghue, “Introduction to non-linear field theory”, Proc. of the Workshop on Effective Field Theories of the Standard Model, Dobogókő, Hungary, Aug. 1991, Ed. U.-G. Meißner, World Scient. Publ. Co. (Singapore, 1992).
- [45] A.G. Cohen, G. Ecker and A. Pich, Phys. Lett. B304 (1993) 347.
- [46] F.J. Gilman and M.B. Wise, Phys. Rev. D21 (1980) 3150.
- [47] E. Ma and A. Pramudita, Phys. Rev. D24 (1984) 2476.
- [48] J. F. Donoghue, B. R. Holstein and Y.-C. R. Lin, Nucl. Phys. B277 (1986) 651.
- [49] B.R. Martin and E. de Rafael, Nucl. Phys. B8 (1968) 131;  
P. Pavlopoulos, in “Flavor Mixing in Weak Interactions”, Ed. L.L. Chau, Ettore Majorana International Science Series (Plenum, New York 1985), Vol. 20, p. 577;  
R. Decker, P. Pavlopoulos and G. Zoupanos, Z. Phys. C28 (1985) 117.
- [50] J.O. Eeg and I. Picek, Phys. Lett. B196 (1987) 391; J.O. Eeg, B. Nizic and I. Picek, Phys. Lett. B244 (1990) 513.
- [51] H.-Y. Cheng, Phys. Lett. B245 (1990) 122.
- [52] J. Gasser and H. Leutwyler, Nucl. Phys. B250 (1985) 465.
- [53] S. Kawabata (KEK), “Physics in two-photon interactions” , in Proc. of the Joint International Lepton-Photon Symposium and Europhysics Conference on High Energy Physics, Geneva, Aug. 1991, Eds. S. Hegarty, K. Potter and E. Quercigh, World Scient. Publ. Co. (Singapore, 1992).
- [54] M.S. Atiya et al. (BNL-E787), Phys. Rev. Lett. 65 (1990) 1188.
- [55] E. Golowich, “Comments on CP violation in rare kaon decays and on the status of the B parameter”, in Proc. 5<sup>th</sup> Moriond Workshop: Flavour Mixing and CP Violation, Ed. J. Tran Thanh Van, Editions Frontières (Gif-sur-Yvette, 1985).

- [56] M. Fukawa et al., “Physics at a  $\phi$  factory: CP and CPT violations in kaon decays”, KEK Report 90-12 .
- [57] G. D’Ambrosio, G. Isidori and A. Pugliese, in this report and references therein.
- [58] F.E. Low, Phys. Rev. 110 (1958) 974.
- [59] P. Heiliger and L.M. Sehgal, Phys. Lett. B307 (1993) 182.
- [60] A. Manohar and H. Georgi, Nucl. Phys. B234 (1984) 189.
- [61] G. D’Ambrosio, M. Miragliuolo and F. Sannino, Z. Phys. C59 (1993) 451.
- [62] G. D’Ambrosio and G. Isidori, Z. Phys. C65 (1995) 649.
- [63] E.J. Ramberg et al. (FNAL–E731), Phys. Rev. Lett. 70 (1993) 2525.
- [64] A.S. Carroll et al., Phys. Lett. 96B (1980) 407.
- [65] E.J. Ramberg, private communication.
- [66] L. Littenberg and G. Valencia, in Ref. [1].
- [67] G. Ecker, J. Gasser, H. Leutwyler, A. Pich and E. de Rafael, Phys. Lett. B223 (1989) 425.
- [68] R.J. Abrams et al., Phys. Rev. Lett. 29 (1972) 1118;  
V.N. Bolotov et al., Sov. J. Nucl. Phys. 45 (1987) 1023.
- [69] C.O. Dib and R.D. Peccei, Phys. Lett. B249 (1990) 325.
- [70] H.-Y. Cheng, Phys. Lett. B315 (1993) 170; Phys. Rev. D49 (1994) 3771;  
N. Paver, Riazuddin, F. Simeoni, Phys. Lett. B316 (1993) 397.
- [71] E.J. Ramberg et al. (FNAL–E731), Phys. Rev. Lett. 70 (1993) 2529.
- [72] G. D’Ambrosio and N. Paver, Phys. Rev. D49 (1994) 4560.
- [73] L.M. Sehgal, Phys. Rev. D7 (1973) 3303.
- [74] G. Ecker, “Chiral realization of the non-leptonic weak interactions”, in Proc. 24<sup>th</sup> Int. Symposium on the Theory of Elementary Particles, Gosen (Berlin), Ed. G. Weigt (Zeuthen, 1991).
- [75] J. Bijnens, A. Bramon and F. Cornet, Z. Phys. C46 (1990) 599.
- [76] G.D. Barr et al. (CERN–NA31), Phys. Lett. B240 (1990) 283.
- [77] L. Bergström, E. Massó and P. Singer, Phys. Lett. 131B (1983) 229.

- [78] K.E. Ohl et al. (BNL–E845), Phys. Rev. Lett. 65 (1990) 1407.
- [79] G. Ecker and A. Pich, Nucl. Phys. B366 (1991) 189.
- [80] T. Akagi et al. (KEK–137), Phys. Rev. Lett. 67 (1991) 2618.
- [81] A.P. Heinson et al. (BNL–E791), Phys. Rev. D44 (1991) R1.
- [82] L. Bergström, E. Massó and P. Singer, Phys. Lett. B249 (1990) 141;  
G. Bélanger and C.Q. Geng, Phys. Rev. D43 (1991) 140;  
P. Ko, Phys. Rev. D45 (1992) 174.
- [83] G. Ecker, A. Pich and E. de Rafael, Nucl. Phys. B291 (1987) 692.
- [84] C. Alliegro et al., Phys. Rev. Lett. 68 (1992) 278.
- [85] M.J. Savage and M.B. Wise, Phys. Lett. 250B (1990) 151;  
M. Lu, M.B. Wise and M.J. Savage, Phys. Rev. D46 (1992) 5026.
- [86] L.M. Sehgal and M. Wanninger, Phys. Rev. D46 (1992) 1035; E ibid. D46 (1992) 5209.
- [87] P. Heiliger and L.M. Sehgal, Phys. Rev. D48 (1993) 4146.
- [88] L. Littenberg, Phys. Rev. D39 (1989) 3322.
- [89] J.F. Donoghue and F. Gabbiani, Phys. Rev. D51 (1995) 2187.